

COSMO: A conic operator splitting method for convex conic problems

Michael Garstka*

Mark Cannon*

Paul Goulart *

September 10, 2020

Abstract

This paper describes the Conic Operator Splitting Method (COSMO) solver, an operator splitting algorithm for convex optimisation problems with quadratic objective function and conic constraints. At each step the algorithm alternates between solving a quasi-definite linear system with a constant coefficient matrix and a projection onto convex sets. The low per-iteration computational cost makes the method particularly efficient for large problems, e.g. semidefinite programs that arise in portfolio optimisation, graph theory, and robust control. Moreover, the solver uses chordal decomposition techniques and a new clique merging algorithm to effectively exploit sparsity in large, structured semidefinite programs. A number of benchmarks against other state-of-the-art solvers for a variety of problems show the effectiveness of our approach. Our Julia implementation is open-source, designed to be extended and customised by the user, and is integrated into the Julia optimisation ecosystem.

1 Introduction

We consider convex optimisation problems in the form

$$\begin{aligned} & \text{minimize} && f(x) \\ & \text{subject to} && g_i(x) \leq 0, \quad i = 1, \dots, l \\ & && h_i(x) = 0, \quad i = 1, \dots, k, \end{aligned} \tag{1}$$

where we assume that both the objective function $f : \mathbb{R}^n \rightarrow \mathbb{R}$ and the inequality constraint functions $g_i : \mathbb{R}^n \rightarrow \mathbb{R}$ are convex, and that the equality constraints $h_i(x) := a_i^\top x - b_i$ are affine. We will denote an optimal solution to this problem (if it exists) as x^* . Convex optimisation problems feature heavily in a wide range of research areas and industries, including problems

*The authors are with the Department of Engineering Science, University of Oxford, Oxford, OX1 3PJ, UK. Email: {michael.garstka, mark.cannon, paul.goulart}@eng.ox.ac.uk

in machine learning [CV95], finance [BBD⁺17], optimal control [BEGFB94], and operations research [BHH01]. Concrete examples of problems fitting the general form (1) include linear programming (LP), convex quadratic programming (QP), second-order cone programming (SOCP), and semidefinite programming (SDP) problems. Methods to solve each of these standard problem classes are well known and a number of open- and closed-source solvers are widely available. However, the trend for data and training sets of increasing size in decision making problems and machine learning poses a challenge for state-of-the-art software.

Algorithms for LPs were first used to solve military planning and allocation problems in the 1940s [Dan63]. In 1947 Danzig developed the simplex method that solves LPs by searching for the optimal solution along the vertices of the inequality polytope. Extensions to the method led to the general field of *active-set methods* [Wol59] that are able to solve both LPs and QPs, and which search for an optimal point by iteratively constructing a set of active constraints. Although often efficient in practice, a major theoretical drawback is that the worst-case complexity increases exponentially with the problem size [WN99].

The most common approach taken by modern convex solvers is the *interior-point method* [WN99], which stems from Karmarkar's original projective algorithm [Kar84], and is able to solve both LPs and QPs in polynomial time. Interior point methods have since been extended to problems with positive semidefinite (PSD) constraints in [HRVW96] and [AHO98]. The primal-dual interior point methods apply variants of Newton's method to iteratively find a solution to a set of optimality KKT conditions. At each iteration the algorithm alternates between a Newton step that involves factoring a Jacobian matrix and a line search to determine the magnitude of the step to ensure a feasible iterate. Most notably, the Mehrotra predictor-corrector method in [Meh92] forms the basis of several implementations because of its strong practical performance [Wri97]. However, interior-point methods typically do not scale well for very large problems since the Jacobian matrix has to be calculated and factored at each step.

Two main approaches to overcome this limitation are active research areas. Firstly, a renewed focus on first-order methods with computationally cheaper per-iteration-cost, and secondly the exploitation of sparsity in the problem data. First-order methods are known to handle larger problems well at the expense of reduced accuracy compared to interior-point methods. In the 1960s Everett [Eve63] proposed a dual decomposition method that allows one to decompose a separable objective function, making each iteration cheaper to compute. Augmented Lagrangian methods by Miele ([MCIL71, MCL71, MMLC72]), Hestenes [Hes69], and Powell [Pow69] are more robust and helped to remove the strict convexity conditions on problems, while losing the decomposition property. By splitting the objective function, the alternating direction method of multipliers (ADMM), first described in [GM75], allowed the advantages of dual decomposition to be combined with the superior convergence and robustness of augmented Lagrangian methods. Subsequently, it was shown that ADMM can be analysed from the perspective of monotone operators and that it is a special case of Douglas-Rachford splitting [Eck89] as well as of the proximal point algorithm in [Roc76], which allowed further insight into the method.

ADMM methods are simple to implement and computationally cheap, even for large problems.

However, they tend to converge slowly to a high accuracy solution and the detection of infeasibility is more involved compared to interior-point methods. They are therefore most often used in applications where a modestly accurate solution is sufficient [PB⁺14]. Most of the early advances in first-order methods such as ADMM happened in the 1970s/80s long before the demand for large scale optimisation, which may explain why they stayed less well-known and have only recently resurfaced.

A method of exploiting the sparsity pattern of PSD constraints in an interior-point algorithm was developed in [FKMN01]. This work showed that if the coefficient matrices of an SDP exhibit an aggregate sparsity pattern represented by a chordal graph, then both primal and dual problems can be decomposed into a problem with many smaller PSD constraints on the nonzero blocks of the original matrix variable. These blocks are associated with subsets, called *cliques*, of graph vertices. Moreover, it can be advantageous to merge some of these blocks, for example if they overlap significantly. The optimal way to merge the blocks, or equivalently the corresponding graph cliques, after the initial decomposition depends on the solver algorithm and is still an open question. Sparsity in SDPs has also been studied for problems with underlying graph structure, e.g. optimal power-flow problems in [MHL13] and graph optimisation problems in [Ali95].

Related Work Widely used solvers for conic problems, especially SDPs, include SeDuMi [Stu99], SDPT3 [TTT99] (both open source, MATLAB), and MOSEK [MOS17] (commercial, C) among others. All of these solvers implement primal-dual interior-point methods.

Both Fukuda [FKMN01] and Sun [SAV14] developed interior-point solvers that exploit chordal sparsity patterns in PSD constraints. Some heuristic methods to merge cliques have been proposed for interior-point methods in [MHL13] and been implemented in the SparseCoLo package [FKK⁺09] and the CHOMPACk package [AV15].

Several solvers based on the ADMM method have been released recently. The solver OSQP [SBG⁺18] is implemented in C and detects infeasibility based on the differences of the iterates [BGSB17], but only solves LPs and QPs. The C-based SCS [OCPB16] implements an operator splitting method that solves the primal-dual pair of conic programs in order to provide infeasibility certificates. The underlying homogeneous self-dual embedding method has been extended by [ZFP⁺19] to exploit sparsity and implemented in the MATLAB solver CDCS. The conic solvers SCS and CDCS are unable to handle quadratic cost functions directly. Instead they are forced to reformulate problem with quadratic objective functions by adding a second-order cone constraint, which increases the problem size. Moreover, they rely on primal-dual formulations to detect infeasibility.

Outline In Section 2 we define the general conic problem format, its dual problem, as well as optimality and infeasibility conditions. Section 3 describes the ADMM algorithm that is used by COSMO. Section 4 explains how to decompose SDPs in a preprocessing step provided the problem data has an aggregated sparsity pattern. In Section 5 we describe a new clique merging strategy and compare it to existing approaches. Implementation details and code related design choices

are discussed in Section 6. Section 7 shows benchmark results of COSMO vs. other state-of-the-art solvers on a number of test problems. Section 8 concludes the paper.

Contributions With the solver package described in this paper we make the following contributions:

1. We implement a first-order method for large conic problems that is able to detect infeasibility without the need of a homogeneous self-dual embedding.
2. COSMO directly supports quadratic objective functions, thus reducing overheads for applications with both quadratic objective function and PSD constraints. This also avoids a major disadvantage of conic solvers compared to native QP solvers, i.e no additional matrix factorisation for the conversion is needed and favourable sparsity in the objective can be maintained.
3. Large structured positive semidefinite programs are analysed and, if possible, chordally decomposed. This typically allows one to solve very large sparse and structured problems orders of magnitudes faster than competing solvers. For complex sparsity patterns, further performance improvements are achieved by recombining some of the sub-blocks of the initial decomposition in an optimal way. For this purpose, we propose a new clique graph based merging strategy and compare it to existing heuristic approaches.
4. The open-source solver is written in a modular way in the fast and flexible programming language Julia. The design allows users to extend the solver by specifying a specific linear system solver and by defining their own convex cones or custom projection methods.

Notation The following notation and definitions will be used throughout this paper. Denote the space of real numbers \mathbb{R} , the n -dimensional real space \mathbb{R}^n , the n -dimensional zero cone $\{0\}^n$, the nonnegative orthant \mathbb{R}_+^n , the space of symmetric matrices \mathbb{S}^n , and the set of positive semidefinite matrices \mathbb{S}_+^n .

In some of the following sections matrix data is considered in vectorized form. Denote the vectorization of a matrix X by stacking its columns as $x := \text{vec}(X)$ and the inverse operation as $\text{vec}^{-1}(x) = \text{mat}(x)$. For symmetric matrices it is often computationally beneficial to work only with the upper-triangular elements of the matrix. Denote the transformation of a symmetric matrix $V \in \mathbb{S}^n$ with i,j -th element V_{ij} into a vector of upper-triangular elements as

$$\text{svec}(V) := \left[V_{11}, \sqrt{2}V_{12}, V_{22}, \sqrt{2}V_{13}, \sqrt{2}V_{23}, V_{33}, \sqrt{2}V_{14}, \dots, V_{nn} \right]^\top. \quad (2)$$

Here the scaling factor of $\sqrt{2}$ preserves the matrix inner product, i.e. $\text{tr}(AB) = \text{svec}(A)^\top \text{svec}(B)$ for symmetric matrices $A, B \in \mathbb{S}^n$. The inverse operation is denoted by $\text{svec}^{-1}(s) =: \text{smat}(s)$. Denote the Kronecker product of two matrices A and B as $A \otimes B$. The Frobenius norm of a matrix A is given by $\|A\|_F = (\sum_{ij} |a_{ij}|^2)^{1/2}$.

Sometimes we consider positive semidefinite constraints in vector form, so we define the space of vectorized symmetric positive semidefinite matrices as

$$\mathcal{S}_+^n := \left\{ s \in \mathbb{R}^{\frac{n(n+1)}{2}} : \text{smat}(s) \in \mathbb{S}_+^n \right\}.$$

For a convex cone \mathcal{K} denote the *polar cone* by

$$\mathcal{K}^\circ := \left\{ y \in \mathbb{R}^n \mid \sup_{x \in \mathcal{K}} \langle x, y \rangle \leq 0 \right\},$$

the *normal cone* of \mathcal{K} by

$$N_{\mathcal{K}}(x) := \left\{ y \in \mathbb{R}^n \mid \sup_{\bar{x} \in \mathcal{K}} \langle \bar{x} - x, y \rangle \leq 0 \right\},$$

and, following [Roc70], the *recession cone* of \mathcal{K} by

$$\mathcal{K}^\infty := \{ y \in \mathbb{R}^n \mid x + ay \in \mathcal{K}, \forall x \in \mathcal{K}, \forall a \geq 0 \}.$$

The *proximal operator* of a convex, closed and proper function $f: \mathbb{R}^n \rightarrow \mathbb{R}$ is given by

$$\text{prox}_f(x) := \underset{y}{\text{argmin}} \left\{ f(y) + \frac{1}{2} \|y - x\|_2^2 \right\}.$$

We denote the *indicator function* of a nonempty, closed convex set $\mathcal{C} \subseteq \mathbb{R}^n$ by

$$I_{\mathcal{C}}(x) := \begin{cases} 0 & x \in \mathcal{C} \\ +\infty & \text{otherwise,} \end{cases}$$

and the *projection* of $x \in \mathbb{R}^n$ onto \mathcal{C} by:

$$\Pi_{\mathcal{C}}(x) := \underset{y \in \mathcal{C}}{\text{argmin}} \|x - y\|_2^2.$$

We further denote the *support function* of \mathcal{C} by:

$$\sigma_{\mathcal{C}}(x) := \sup_{y \in \mathcal{C}} \langle x, y \rangle.$$

2 Conic Problems

We will address convex optimisation problems with a quadratic objective function and a number of conic constraints in the form:

$$\begin{aligned} & \text{minimize} && \frac{1}{2} x^\top P x + q^\top x \\ & \text{subject to} && A x + s = b \\ & && s \in \mathcal{K}, \end{aligned} \tag{3}$$

where $x \in \mathbb{R}^n$ is the primal *decision variable* and $s \in \mathbb{R}^m$ is the primal *slack variable*. The objective function is defined by positive semidefinite matrix $P \in \mathbb{S}_+^n$ and vector $q \in \mathbb{R}^n$. The constraints are defined by matrix $A \in \mathbb{R}^{m \times n}$, vector $b \in \mathbb{R}^m$ and a non-empty, closed, convex cone \mathcal{K} which itself can be a Cartesian product of cones in the form

$$\mathcal{K} = \mathcal{K}_1^{m_1} \times \mathcal{K}_2^{m_2} \times \cdots \times \mathcal{K}_N^{m_N}, \quad (4)$$

with cone dimensions $\sum_{i=1}^N m_i = m$. Note that any LP, QP, SOCP, or SDP can be written in the form (3) using an appropriate choice of cones, as well as problems involving the power or exponential cones and their duals.

The dual problem associated with (3) is given by:

$$\begin{aligned} & \text{maximize} && -\frac{1}{2}x^\top Px + b^\top y - \sigma_{\mathcal{K}}(y) \\ & \text{subject to} && Px - A^\top y = -q \\ & && y \in (\mathcal{K}^\infty)^\circ, \end{aligned} \quad (5)$$

with dual variable $y \in \mathbb{R}^m$.

The conditions for optimality (assuming linear independence constraint qualification) follow from the Karush-Kuhn-Tucker (KKT) conditions:

$$Ax + s = b, \quad (6a)$$

$$Px + q - A^\top y = 0, \quad (6b)$$

$$s \in \mathcal{K}, \quad y \in (\mathcal{K}^\infty)^\circ. \quad (6c)$$

Assuming strong duality, if there exists a $x^* \in \mathbb{R}^n$, $s^* \in \mathbb{R}^m$, and $y^* \in \mathbb{R}^m$ that fulfil (6a)–(6c) then the pair (x^*, s^*) is called the primal solution and y^* is called the dual solution of problem (3).

2.1 Infeasibility certificates

Primal and dual infeasibility conditions were developed for ADMM in [BGSB17]. These conditions are directly applicable to problems of the form (3). To simplify the notation of the conditions, define the cone $\bar{\mathcal{K}} := -\mathcal{K} + \{b\}$. Then, the following sets provide certificates for primal and dual infeasibility:

$$\mathcal{P} = \{x \in \mathbb{R}^n \mid Px = 0, Ax \in \bar{\mathcal{K}}^\infty, \langle q, x \rangle < 0\}. \quad (7)$$

$$\mathcal{D} = \{y \in \mathbb{R}^m \mid A^\top y = 0, \sigma_{\bar{\mathcal{K}}}(y) < 0\}, \quad (8)$$

The existence of some $y \in \mathcal{D}$ certifies that problem (3) is primal infeasible, while the existence of some $x \in \mathcal{P}$ certifies dual infeasibility.

3 ADMM Algorithm

We use the same splitting as in [SBG⁺18] to transform problem (3) into standard ADMM format. The problem is rewritten by introducing the dummy variables $\tilde{x} = x$ and $\tilde{s} = s$:

$$\begin{aligned} & \text{minimize } \frac{1}{2}\tilde{x}^\top P\tilde{x} + q^\top \tilde{x} + I_{Ax+s=b}(\tilde{x}, \tilde{s}) + I_{\mathcal{K}}(s) \\ & \text{subject to } (\tilde{x}, \tilde{s}) = (x, s), \end{aligned} \quad (9)$$

where the indicator functions of the sets $\{(x, s) \in \mathbb{R}^n \times \mathbb{R}^m \mid Ax + s = b\}$ and \mathcal{K} were used to move the constraints of (3) into the objective function. The augmented Lagrangian of (9) is given by

$$\begin{aligned} L(x, s, \tilde{x}, \tilde{s}, \lambda, y) &= \frac{1}{2}\tilde{x}^\top P\tilde{x} + q^\top \tilde{x} + \mathcal{I}_{Ax+s=b}(\tilde{x}, \tilde{s}) + \mathcal{I}_{\mathcal{K}}(s) \\ &+ \frac{\sigma}{2} \left\| \tilde{x} - x + \frac{1}{\sigma}\lambda \right\|_2^2 + \frac{\rho}{2} \left\| \tilde{s} - s + \frac{1}{\rho}y \right\|_2^2, \end{aligned} \quad (10)$$

with step size parameters $\rho > 0$ and $\sigma > 0$ and dual variables $\lambda \in \mathbb{R}^n$ and $y \in \mathbb{R}^m$. The corresponding ADMM iteration is given by:

$$(\tilde{x}^{k+1}, \tilde{s}^{k+1}) = \underset{\tilde{x}, \tilde{s}}{\operatorname{argmin}} L(\tilde{x}, \tilde{s}, x^k, s^k, \lambda^k, y^k), \quad (11a)$$

$$x^{k+1} = \alpha \tilde{x}^{k+1} + (1 - \alpha)x^k + \frac{1}{\sigma}\lambda^k, \quad (11b)$$

$$s^{k+1} = \underset{s}{\operatorname{argmin}} \frac{\rho}{2} \left\| \alpha \tilde{s}^{k+1} + (1 - \alpha)s^k - s + \frac{1}{\rho}y^k \right\|_2^2 + I_{\mathcal{K}}(s), \quad (11c)$$

$$\lambda^{k+1} = \lambda^k + \sigma (\alpha \tilde{x}^{k+1} + (1 - \alpha)x^k - x^{k+1}), \quad (11d)$$

$$y^{k+1} = y^k + \rho (\alpha \tilde{s}^{k+1} + (1 - \alpha)s^k - s^{k+1}), \quad (11e)$$

where we relaxed the z -update and the dual variable update with relaxation parameter $\alpha \in (0, 2)$ according to [EB92]. Notice from (11b) and (11d) that the dual variable corresponding to the constraint $x = \tilde{x}$ satisfies $\lambda^k = 0$ for all k .

3.1 Solution of the equality constrained QP

The minimization problem in (11a) has the form of an equality-constrained quadratic program:

$$\begin{aligned} & \text{minimize } \frac{1}{2}\tilde{x}^\top P\tilde{x} + q^\top \tilde{x} + \frac{\sigma}{2} \left\| \tilde{x} - x^k \right\|_2^2 + \frac{\rho}{2} \left\| \tilde{s} - s^k + \frac{1}{\rho}y^k \right\|_2^2 \\ & \text{subject to } A\tilde{x} + \tilde{s} = b. \end{aligned} \quad (12)$$

The solution of (12) can be obtained by solving a single linear system. The corresponding Lagrangian is given by:

$$\mathcal{L}(\tilde{x}, \tilde{s}, \nu) = \frac{1}{2}\tilde{x}^\top P\tilde{x} + q^\top \tilde{x} + \frac{\sigma}{2} \left\| \tilde{x} - x^k \right\|_2^2 + \frac{\rho}{2} \left\| \tilde{s} - s^k + \frac{1}{\rho}y^k \right\|_2^2 + \nu^\top (A\tilde{x} + \tilde{s} - b), \quad (13)$$

where the Lagrangian multiplier $\nu \in \mathbb{R}^m$ accounts for the equality-constraint $Ax + s = b$. Thus, the KKT optimality conditions for this equality constrained QP are given by:

$$\frac{\partial \mathcal{L}}{\partial \tilde{x}} = P\tilde{x}^{k+1} + q + \sigma(\tilde{x}^{k+1} - x^k) + A^\top \nu^{k+1} = 0, \quad (14)$$

$$\frac{\partial \mathcal{L}}{\partial \tilde{s}} = \rho \left(\tilde{s}^{k+1} - s^k + \frac{1}{\rho} y^k \right) + \nu^{k+1} = 0, \quad (15)$$

$$A\tilde{x}^{k+1} + \tilde{s}^{k+1} - b = 0. \quad (16)$$

Elimination of \tilde{s}^{k+1} from these equations leads to the linear system:

$$\begin{bmatrix} P + \sigma I & A^\top \\ A & -\frac{1}{\rho} I \end{bmatrix} \begin{bmatrix} \tilde{x}^{k+1} \\ \nu^{k+1} \end{bmatrix} = \begin{bmatrix} -q + \sigma x^k \\ b - s^k + \frac{1}{\rho} y^k \end{bmatrix} \quad (17)$$

with

$$\tilde{s}^{k+1} = s^k - \frac{1}{\rho} (\nu^{k+1} + y^k). \quad (18)$$

Note that the introduction of the dummy variable \tilde{x} led to the term σI in the upper-left corner of the coefficient matrix in (17). Consequently, the coefficient matrix in (17) is always quasi-definite [Van95], i.e. it always has a positive definite upper-left block and a negative definite lower-right block, and is therefore full rank even when $P = 0$ or A is rank deficient. Following [Van95] the left hand side of (17) always has a well-defined LDL^\top factorization with a diagonal D .

3.2 Projection step

As shown in [PB⁺14] the minimization problem in (11c) can be interpreted as the ρ -weighted proximal operator of the indicator function $I_{\mathcal{K}}$. It is therefore equivalent to the Euclidean projection $\Pi_{\mathcal{K}}$ onto the cone \mathcal{K} , i.e.

$$s^{k+1} = \Pi_{\mathcal{K}} \left(\alpha \tilde{s}^{k+1} + (1 - \alpha) s^k + \frac{1}{\rho} y^k \right). \quad (19)$$

If \mathcal{K} is a Cartesian product of cones as in (4) this projection is equivalent to the projection of the relevant components of the argument of $\Pi_{\mathcal{K}}(\cdot)$ onto each cone \mathcal{K}_i . A problem with N SDP constraints therefore requires N projections, but, since each of these operates on an independent segment of the input vector, they can be performed in parallel.

3.3 Algorithm steps

The calculations performed at each iteration are summarized in Algorithm 1. Observe that the coefficient matrix of the linear system in (17) is constant, so that one can precompute and cache the LDL^\top factorization and efficiently evaluate line 2 with changing right hand sides. A refactorization is only necessary if the step size parameters ρ and σ are updated.

Algorithm 1: ADMM iteration

Input : initial values x^0, s^0, y^0 , problem data P, q, A, b , and parameters $\sigma > 0, \rho > 0, \alpha \in (0, 2)$

1 Do

2 | $(\tilde{x}^{k+1}, \nu^{k+1}) \leftarrow$ solve linear system (17);
3 | $\tilde{s}^{k+1} \leftarrow s^k - \frac{1}{\rho}(\nu^{k+1} + y^k);$
4 | $x^{k+1} \leftarrow \alpha\tilde{x}^{k+1} + (1 - \alpha)x^k;$
5 | $s^{k+1} \leftarrow \Pi_{\mathcal{K}} \left(\alpha\tilde{s}^{k+1} + (1 - \alpha)s^k + \frac{1}{\rho}y^k \right);$
6 | $y^{k+1} \leftarrow y^k + \rho(\alpha\tilde{s}^{k+1} + (1 - \alpha)s^k - s^{k+1});$
7 **while** *termination criteria not satisfied*;

Lines 3, 4, and 6 are computationally inexpensive since they involve only vector addition and scalar-vector multiplication. The projection in line 5 is crucial to the performance of the algorithm depending on the particular cones employed in the model: projections onto the zero-cone or the nonnegative orthant are inexpensive, while a projection onto the positive-semidefinite cone of dimension N involves an eigenvalue decomposition. Since direct methods for eigen-decompositions have a complexity of approximately $\mathcal{O}(N^3)$, this turns line 5 into the most computationally expensive operation of the algorithm for large SDPs, and improving the efficiency of this step will be the objective of much of Sections 4 and 5.

3.4 Algorithm convergence

For feasible problems, Algorithm 1 produces a sequence of iterates (x^k, s^k, y^k) that converges to a limit satisfying the optimality conditions in (6) as $k \rightarrow \infty$. The authors in [SBG⁺18] show convergence of Algorithm 1 by applying the Douglas-Rachford splitting to a problem reformulation.

In the Douglas-Rachford formulation, lines 5 and 6 become projections onto \mathcal{K} and \mathcal{K}° respectively, so that the conic constraints in (6c) always hold. Furthermore, convergence of the residual iterates in (6a)–(6b) can be concluded from the convergence of the splitting variables

$$x^k - \tilde{x}^k \rightarrow 0, \quad s^k - \tilde{s}^k \rightarrow 0, \quad (20)$$

which generally holds for Douglas-Rachford splitting [BC11].

For infeasible problems, [BGSB17] showed that Algorithm 1 leads to convergence of the successive differences between iterates

$$\delta x^k = x^k - x^{k-1}, \quad \delta s^k = s^k - s^{k-1}, \quad \delta y^k = y^k - y^{k-1}. \quad (21)$$

For primal infeasible problems $\delta y = \lim_{k \rightarrow \infty} \delta y^k$ will satisfy condition (8), whereas for dual infeasible problems $\delta x = \lim_{k \rightarrow \infty} \delta x^k$ is a certificate of (7).

3.5 Scaling the problem data

The rate of convergence of ADMM and other first-order methods depends in practice on the scaling of the problem data; see [GB14]. Particularly for badly conditioned problems, this suggests a preprocessing step where the problem data is scaled in order to improve convergence. For certain problem classes an optimal scaling has been found, see [GB14, GB15, Gre97]. However, the computation of the optimal scaling is often more complicated than solving the original problem. Consequently, most algorithms rely on heuristic methods such as matrix equilibration.

We scale the equality constraints by diagonal positive definite matrices D and U . The scaled form of (3) is given by:

$$\begin{aligned} \text{minimize} \quad & \frac{1}{2} \hat{x}^\top \hat{P} \hat{x} + \hat{q}^\top \hat{x} \\ \text{subject to} \quad & \hat{A} \hat{x} + \hat{s} = \hat{b}, \\ & \hat{s} \in UK, \end{aligned} \tag{22}$$

with scaled problem data

$$\hat{P} = DPD, \quad \hat{q} = Dq, \quad \hat{A} = UAD, \quad \hat{b} = Ub, \tag{23}$$

and the scaled convex cone $UK := \{Uv \in \mathbb{R}^m \mid v \in \mathcal{K}\}$. After solving (22) the original solution is obtained by reversing the scaling:

$$x = D\hat{x}, \quad s = U^{-1}\hat{s}, \quad y = U\hat{y}. \tag{24}$$

One heuristic strategy that has been shown to work well in practice is to choose the scaling matrices D and U to equilibrate, i.e. reduce the condition number of, the problem data. The Ruiz equilibration technique described in [Rui01] iteratively scales the rows and columns of a matrix to have an infinity-norm of 1 and converges linearly. We apply the modified Ruiz algorithm shown in Algorithm 2 to reduce the condition number of the symmetric matrix R

$$R = \begin{bmatrix} P & A^\top \\ A & 0 \end{bmatrix} \tag{25}$$

which represents the problem data. Since R is symmetric it suffices to consider the columns $R_{c,i}$ of R . At each iteration the scaling routine calculates the norm of each column. For the columns with norms higher than the tolerance τ scaling vector c is updated with the inverse square root of the norm¹. If the norm is below the tolerance, the corresponding column will be scaled by 1.

Since the matrix U scales the (possibly composite) cone constraint, the scaling must ensure that if $s \in \mathcal{K}$ then $U^{-1}s \in \mathcal{K}$. Let \mathcal{K} be a Cartesian product of N cones as in (4) and partition U into blocks

$$U = \text{diag}(U_1, \dots, U_N), \tag{26}$$

¹For the presented results a value of $\tau = 10^{-6}$ was chosen.

Algorithm 2: Modified Ruiz equilibration

```

1 set  $D = I_n, U = I_m, c = \mathbf{1}_{m+n};$ 
2 Do
3   for  $i = 1, \dots, n + m$  do
4     if  $\|R_{c,i}\|_\infty > \tau$  then
5        $c_i \leftarrow \|R_{c,i}\|_\infty^{-\frac{1}{2}};$ 
6      $\hat{D} = \text{diag}(c_{1:n}), \hat{U} = \text{diag}(c_{n+1:n+m});$ 
7      $D = \hat{D} \cdot D, U = \hat{U} \cdot U;$ 
8      $P = \hat{D}P\hat{D}, A = \hat{U}A\hat{D};$ 
9     assemble  $R;$ 
10 while  $\|\mathbf{1} - c\|_\infty > \text{tol};$ 
11 return  $D, U;$ 

```

with block $U_i \in \mathbb{R}^{m_i \times m_i}$ which scales the constraint corresponding to \mathcal{K}_i . For each cone $\mathcal{K}_i \in \mathbb{R}^{m_i}$ that requires a scalar or symmetric scaling, *e.g.* a second-order cone or positive semidefinite cone, the corresponding block U_i is replaced with

$$U_i^* := u_i I_{m_i}, \quad \text{for } i = 1, \dots, N \quad (27)$$

where the mean value of the diagonal entries of the original block in U , $u_i = \text{tr}(U_i)/m_i$, was chosen as a heuristic scaling factor.

3.6 Termination criteria

The termination criteria discussed in this section are based on the unscaled problem data and iterates. Thus, before checking for termination the solver first reverses the scaling according to equations (23)–(24). To measure the progress of the algorithm, we define the primal and dual residuals of the problem as:

$$r_p := Ax + s - b, \quad (28a)$$

$$r_d := Px + q - A^\top y. \quad (28b)$$

According to Section 3.3 of [BPC⁺11] a valid termination criterion is that the size of the norms of the residual iterates in (28) are small. Our algorithm terminates if the residual norms are below the sum of an absolute and a relative tolerance term:

$$\|r_p^k\|_\infty \leq \epsilon_{\text{abs}} + \epsilon_{\text{rel}} \max \{ \|Ax^k\|_\infty, \|s^k\|_\infty, \|b\|_\infty \}, \quad (29a)$$

$$\|r_d^k\|_\infty \leq \epsilon_{\text{abs}} + \epsilon_{\text{rel}} \max \{ \|Px^k\|_\infty, \|q\|_\infty, \|A^\top y^k\|_\infty \}, \quad (29b)$$

where ϵ_{abs} and ϵ_{rel} are user defined tolerances.

Following [BGSB17], the algorithm determines if the one-step differences δx^k and δy^k of the primal and dual variable fulfil the normalized infeasibility conditions (8)–(7) up to certain tolerances $\epsilon_{\text{p,inf}}$ and $\epsilon_{\text{d,inf}}$. The solver returns a primal infeasibility certificate if

$$\|A^\top \delta y^k\|_\infty / \|\delta y^k\|_\infty \leq \epsilon_{\text{p,inf}}, \quad (30\text{a})$$

$$\sigma_{\bar{\mathcal{K}}}(\delta y^k) \leq \epsilon_{\text{p,inf}}, \quad (30\text{b})$$

holds and a dual infeasibility certificate if

$$\|P\delta x^k\|_\infty / \|\delta x^k\|_\infty \leq \epsilon_{\text{d,inf}}, \quad (31\text{a})$$

$$q^\top \delta x^k / \|\delta x^k\|_\infty \leq \epsilon_{\text{d,inf}}, \quad (31\text{b})$$

$$A\delta x^k + v \in \bar{\mathcal{K}}^\infty, \quad (31\text{c})$$

$$\text{with } \|v\|_\infty \leq \epsilon_{\text{d,inf}} \|\delta x^k\|_\infty,$$

holds.

4 Chordal Decomposition

As noted in Section 3.3, for large SDPs the eigen-decomposition in the projection step (19) is the principal performance bottleneck for the algorithm. However, since large-scale SDPs often exhibit a certain structure or sparsity pattern, a sensible strategy is to exploit any such structure to alleviate this bottleneck. If the aggregated sparsity pattern is *chordal*, Agler’s [AHMR88] and Grone’s [GJSW84] theorems can be used to decompose a large PSD constraint into a collection of smaller PSD constraints and additional coupling constraints. The projection step applied to the set of smaller PSD constraints is usually significantly faster than when applied to the original constraint. Since the projections are independent of each other, further performance improvement can be achieved by carrying them out in parallel. Our approach is to apply chordal decomposition to a standard form SDP in the form (3) to produce a decomposed problem, and then transform the resulting decomposed problem back to a problem in the form (3) but with more variables and a collection of smaller PSD cone constraints. This process allows us to apply chordal decomposition as a preprocessing step before the problem is handed to the solver. As discussed in Section 4.2, a chordal sparsity pattern can be imposed on any PSD constraint.

4.1 Graph preliminaries

In the following we define graph-related concepts that are useful to describe the sparsity structure of a problem. A good overview of this topic is given in the survey paper [VA⁺15]. Consider the *undirected graph* $G(V, E)$ with vertex set $V = \{1, \dots, n\}$ and edge set $E \subseteq V \times V$. If all vertices are pairwise adjacent, i.e. $E = \{\{v, u\} \mid v, u \in V, v \neq u\}$, the graph is called *complete*. We follow the convention of [VA⁺15] by defining a *clique* as a subset of vertices $\mathcal{C} \subseteq V$ that

induces a *maximal* complete subgraph of G . The number of vertices in a *clique* is given by the cardinality $|\mathcal{C}|$. A *cycle* is a path of edges (i.e. a sequence of distinct edges) joining a sequence of vertices in which only the first and last vertices are repeated.

The following decomposition theory relies on a subset of graphs that exhibit the important property of *chordality*. A graph G is *chordal* (or *triangulated*) if every cycle of length greater than three has a *chord*, which is an edge between nonconsecutive vertices of the cycle. A non-chordal graph can always be made chordal by adding extra edges.

An undirected graph with n vertices can be used to represent the sparsity pattern of a symmetric matrix $S \in \mathbb{S}^n$. Every nonzero entry $S_{ij} \neq 0$ in the lower triangular part of the matrix introduces an edge $(i, j) \in E$. An example of a sparsity pattern and the associated graph is shown in Figure 1(a–b).

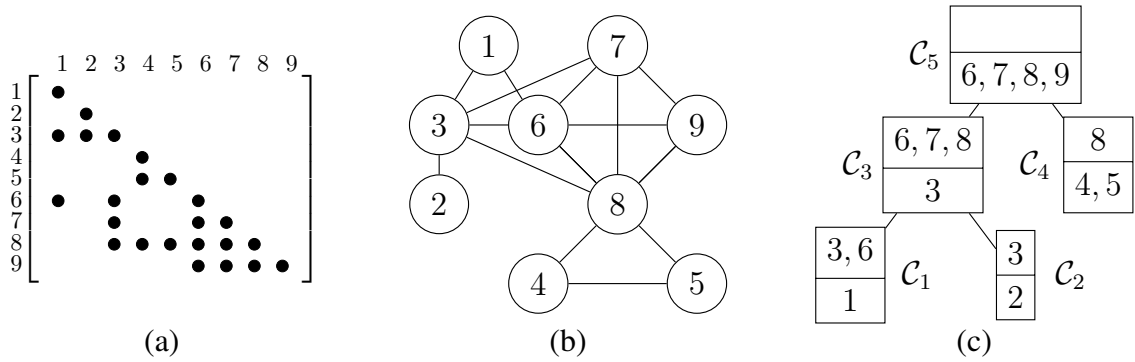


Figure 1: (a) Aggregate sparsity pattern, (b) sparsity graph $G(V, E)$, and (c) clique tree $\mathcal{T}(\mathcal{B}, \mathcal{E})$.

For a given sparsity pattern $G(V, E)$, we define the following symmetric sparse matrix cones:

$$\mathbb{S}^n(E, 0) := \{S \in \mathbb{S}^n \mid S_{ij} = S_{ji} = 0 \text{ if } i \neq j \text{ and } (i, j) \notin E\}, \quad (32)$$

$$\mathbb{S}_+^n(E, 0) := \{S \in \mathbb{S}^n(E, 0) \mid S \succeq 0\}. \quad (33)$$

Given the definition in (32) and a matrix $S \in \mathbb{S}^n(E, 0)$, note that the diagonal entries S_{ii} and the off-diagonal entries S_{ij} with $(i, j) \in E$ may be zero or nonzero. Moreover, we define the cone of positive semidefinite completable matrices as

$$\mathbb{S}_+^n(E, ?) := \left\{ Y \mid \exists \hat{Y} \in \mathbb{S}_+^n, Y_{ij} = \hat{Y}_{ij}, \text{ if } i = j \text{ or } (i, j) \in E \right\}. \quad (34)$$

For a matrix $Y \in \mathbb{S}_+^n(E, ?)$ we can find a positive semidefinite completion by choosing appropriate values for all entries $(i, j) \notin E$. An algorithm to find this completion is described in [VA⁺15]. An important structure that conveys a lot of information about the nonzero blocks of a matrix, or equivalently the cliques of a chordal graph, is the *clique tree* (or *junction tree*). For a chordal graph G let $\mathcal{B} = \{\mathcal{C}_1, \dots, \mathcal{C}_p\}$ be the set of cliques. The clique tree $\mathcal{T}(\mathcal{B}, \mathcal{E})$ is formed by taking the cliques as vertices and by choosing edges from $\mathcal{E} \subseteq \mathcal{B} \times \mathcal{B}$ such that the tree satisfies the *running-intersection property*:

Definition 4.1 (Running intersection property).

For each pair of cliques $\mathcal{C}_i, \mathcal{C}_j \in \mathcal{B}$, the intersection $\mathcal{C}_i \cap \mathcal{C}_j$ is contained in all the cliques on the path in the clique tree connecting \mathcal{C}_i and \mathcal{C}_j .

This property is also referred to as the *clique-intersection property* in [NFF⁺03] and the *induced subtree property* in [VA⁺15]. For a given chordal graph, a clique tree can be computed using the algorithm described in [PS90]. The clique tree for an example sparsity pattern is shown in Figure 1(c).

In a *post-ordered* clique tree the descendants of a node are given consecutive numbers, and a suitable post-ordering can be found via depth-first search. For a clique \mathcal{C}_ℓ we refer to the first clique encountered on the path to the root as its *parent clique* \mathcal{C}_{par} . Conversely \mathcal{C}_ℓ is called the *child* of \mathcal{C}_{par} . If two cliques have the same parent clique we refer to them as *siblings*.

We define the function $\text{par} : 2^V \rightarrow 2^V$ and the multivalued function $\text{ch} : 2^V \rightrightarrows 2^V$ such that $\text{par}(\mathcal{C}_\ell)$ and $\text{ch}(\mathcal{C}_\ell)$ return the parent clique and set of child cliques of \mathcal{C}_ℓ , respectively, where 2^V is the power set (set of all subsets) of V .

Note that each clique in Figure 1(c) has been partitioned into two sets. The upper row represents the *separators* $\eta_\ell = \mathcal{C}_\ell \cap \text{par}(\mathcal{C}_\ell)$, i.e. all clique elements that are also contained in the parent clique. We call the sets of the remaining vertices shown in the lower rows the *clique residuals* or *supernodes* $\nu_\ell = \mathcal{C}_\ell \setminus \eta_\ell$. Keeping track of which vertices in a clique belong to the supernode and the separator is useful as the information is needed to perform a positive semidefinite completion. Following the authors in [HS12], we say that two cliques $\mathcal{C}_i, \mathcal{C}_j$ form a separating pair $\mathcal{P}_{ij} = \{\mathcal{C}_i, \mathcal{C}_j\}$ if their intersection is non-empty and if every path in the underlying graph G from a vertex $\mathcal{C}_i \setminus \mathcal{C}_j$ to a vertex $\mathcal{C}_j \setminus \mathcal{C}_i$ contains a vertex of the intersection $\mathcal{C}_i \cap \mathcal{C}_j$.

4.2 Agler's and Grone's theorems

To explain how the concepts in the previous section can be used to decompose a positive semidefinite constraint, we first consider an SDP in standard primal form:

$$\begin{aligned} & \text{minimize} && \langle C, X \rangle \\ & \text{subject to} && \langle A_k, X \rangle = b_k, \quad k = 1, \dots, m \\ & && X \in \mathbb{S}_+^n, \end{aligned} \tag{35}$$

with variable X and coefficient matrices $A_k, C \in \mathbb{S}^n$. The corresponding dual problem is

$$\begin{aligned} & \text{maximize} && b^\top y \\ & \text{subject to} && \sum_{k=1}^m A_k y_k + S = C \\ & && S \in \mathbb{S}_+^n, \end{aligned} \tag{36}$$

with dual variable $y \in \mathbb{R}^m$ and slack variable S . Let us assume that the problem matrices in (35) and (36) each have their own sparsity pattern

$$A_k \in \mathbb{S}^n(E_{A_k}, 0) \text{ and } C \in \mathbb{S}^n(E_C, 0).$$

The *aggregate sparsity* of the problem is given by the graph $G(V, E)$ with edge set

$$E = E_{A_1} \cup E_{A_2} \cup \dots \cup E_{A_m} \cup E_C.$$

In general $G(V, E)$ will not be chordal, but a *chordal extension* can be found by adding edges to the graph. We denote the extended graph as $G(V, \bar{E})$, where $E \subseteq \bar{E}$. Finding the minimum number of additional edges required to make the graph chordal is an NP-complete problem [Yan81]. Consider a 0–1 matrix M with edge set E . A commonly used heuristic method to compute the chordal extension is to perform a symbolic Cholesky factorisation of M [FKMN01], with the edge set of the Cholesky factor then providing the chordal extension \bar{E} . To simplify the notation in the remainder of the article, we henceforward assume that E represents a chordal graph or has been appropriately extended.

Using the aggregate sparsity of the problem we can modify the constraints on the matrix variables in (35) and (36) to be in the respective sparse positive semidefinite matrix spaces:

$$X \in \mathbb{S}_+^n(E, ?) \text{ and } S \in \mathbb{S}_+^n(E, 0). \quad (37)$$

We further define the entry-selector matrices $T_\ell \in \mathbb{R}^{|\mathcal{C}_\ell| \times n}$ for a clique \mathcal{C}_ℓ as

$$(T_\ell)_{ij} := \begin{cases} 1, & \text{if } \mathcal{C}_\ell(i) = j \\ 0, & \text{otherwise,} \end{cases} \quad (38)$$

where $\mathcal{C}_\ell(i)$ is the i th vertex of \mathcal{C}_ℓ . We can express the constraints in (37) in terms of multiple smaller coupled constraints using Grone's and Agler's theorems.

Theorem 1 (Grone's theorem [GJSW84]). *Let $G(V, E)$ be a chordal graph with a set of maximal cliques $\{\mathcal{C}_1, \dots, \mathcal{C}_p\}$. Then $X \in \mathbb{S}_+^n(E, ?)$ if and only if*

$$X_\ell = T_\ell X T_\ell^\top \in \mathbb{S}_+^{|\mathcal{C}_\ell|}, \quad (39)$$

for all $\ell = 1, \dots, p$.

Applying this theorem to (35) while restricting X to the positive semidefinite completable matrix cone as in (37) yields the decomposed problem:

$$\begin{aligned} & \text{minimize} && \langle C, X \rangle \\ & \text{subject to} && \langle A_k, X \rangle = b_k, \quad k = 1, \dots, m \\ & && X_\ell = T_\ell X T_\ell^\top, \quad \ell = 1, \dots, p \\ & && X_\ell \in \mathbb{S}_+^{|\mathcal{C}_\ell|}, \quad \ell = 1, \dots, p, \end{aligned} \quad (40)$$

For the dual problem we utilise Agler's theorem, which is the dual to Theorem 1:

Theorem 2 (Agler’s theorem [AHMR88]). *Let $G(V, E)$ be a chordal graph with a set of maximal cliques $\{C_1, \dots, C_p\}$. Then $S \in \mathbb{S}_+^n(E, 0)$ if and only if there exist matrices $S_\ell \in \mathbb{S}_+^{|C_\ell|}$ for $\ell = 1, \dots, p$ such that*

$$S = \sum_{\ell=1}^p T_\ell^\top S_\ell T_\ell. \quad (41)$$

Note that the matrices T_ℓ serve to extract the submatrix S_ℓ such that $S_\ell = T_\ell S T_\ell^\top$ has rows and columns corresponding to the vertices of the clique C_ℓ . With this theorem, we transform the dual form SDP in (36) with the restriction on S in (37) to arrive at:

$$\begin{aligned} & \text{maximize} && b^\top y \\ & \text{subject to} && \sum_{k=1}^m A_k y_k + \sum_{\ell=1}^p T_\ell^\top S_\ell T_\ell = C \\ & && S_\ell \in \mathbb{S}_+^{|C_\ell|}, \quad \ell = 1, \dots, p. \end{aligned} \quad (42)$$

4.3 Returning a decomposed problem into standard SDP form

After the decomposition results of Section 4.2 have been applied, the SDP problem (42) has to be transformed back into standard form (3). For the undecomposed problem in (36), this is achieved by first relabeling y as x . We then choose $P = 0_{n \times n}$, $q = -b$, define $A = [\text{svec}(A_1), \dots, \text{svec}(A_m)]$, $b = \text{svec}(C)$ and $s = \text{svec}(S)$.

To transform the decomposed dual problem (42), we will make use of the fact that the decision variable $S \in \mathbb{S}^n$ and all the submatrices S_ℓ are symmetric and consider instead $s_\ell = \text{svec}(S_\ell)$. The main challenge is to keep track of the overlapping entries in the individual blocks and ensure they sum to the original entry in S . Different possible transformations achieving this are described in [KKMY11].

All the necessary information about the overlapping entries is stored in the clique tree $\mathcal{T}(\mathcal{B}, \mathcal{E})$ that represents the sparsity pattern of S . We assume that the clique tree is post-ordered with cliques C_1, \dots, C_p . Define a vector to represent slack variables for overlapping entries $\theta := [\theta_1, \dots, \theta_{n_o}]^\top$, where $n_o := \sum_{\ell=1}^p \frac{|\eta_\ell|(|\eta_\ell|+1)}{2}$ is the total number of overlapping entries in the upper triangle of the sparsity pattern. The s vector of the decomposed problem is created by stacking the vectorized subblocks s_ℓ according to the postordering of the clique tree. Define $\omega(i, j, \ell)$ as the index of s corresponding to the (i, j) th element of block S_ℓ . The equality constraint in problem (42) can be represented in the equivalent standard form (3) as:

$$\left[\begin{array}{ccc|c} \text{svec}(\tilde{A}_1^1) & \cdots & \text{svec}(\tilde{A}_m^1) & \\ \vdots & \ddots & \vdots & \\ \text{svec}(\tilde{A}_1^p) & \cdots & \text{svec}(\tilde{A}_m^p) & \end{array} \right] L \begin{bmatrix} x \\ \theta \end{bmatrix} + \begin{bmatrix} s_1 \\ s_2 \\ \vdots \\ s_p \end{bmatrix} = \begin{bmatrix} \text{svec}(\tilde{B}^1) \\ \vdots \\ \text{svec}(\tilde{B}^p) \end{bmatrix}, \quad (43)$$

with

$$\tilde{A}_{k,ij}^\ell := \begin{cases} A_{k,ij}^\ell & \text{if } (i, j) \notin \text{sep}(\mathcal{C}_\ell) \\ 0 & \text{otherwise,} \end{cases} \quad \tilde{B}_{ij}^\ell := \begin{cases} B_{ij}^\ell & \text{if } (i, j) \notin \text{sep}(\mathcal{C}_\ell) \\ 0 & \text{otherwise.} \end{cases} \quad (44)$$

The matrices \tilde{A}_k^ℓ and \tilde{B}^ℓ take on the values of A_k and B in the locations corresponding to the elements in the submatrix S_ℓ . If a matrix entry of clique \mathcal{C}_ℓ in $A_{k,ij}^\ell$ and B_{ij}^ℓ is overlapped by an entry of the parent clique, i.e. both (i, j) are included in $\text{sep}(\mathcal{C}_\ell)$, it is set to zero. Each column of the linking matrix $L \in \mathbb{R}^{m_d \times n_o}$ links one overlapping entry in the clique tree. L is generated by first collecting all the matrix indices $(i, j)_\ell$ of the separators $\text{sep}(\mathcal{C}_\ell)$ in the clique tree:

$$O := \bigcup_{\ell=1}^p \{(i, j)_\ell \in \text{sep}(\mathcal{C}_\ell) \mid i \leq j\}. \quad (45)$$

Then L is constructed column-by-column, each representing one overlapping entry. The column vector l_c is equal to 1 in the row r corresponding to the $(i, j)_\ell$ -th entry of S_ℓ and -1 in the row corresponding to the same entry of the parent block S_k , where $\mathcal{C}_\ell = \text{ch}(\mathcal{C}_k)$. Thus, each element in l_c is defined by:

$$l_{rc} := \begin{cases} 1 & \text{if } r = \omega(i, j, \ell) \\ -1 & \text{if } r = \omega(i, j, \text{par}(\ell)) \\ 0 & \text{otherwise,} \end{cases} \quad \text{for each } (i, j)_\ell \in O. \quad (46)$$

As an example consider a problem with $m = 1$ and $p = 3$ and the simple sparsity pattern and clique tree given by:

$$S = \begin{bmatrix} 11 - 11x & 12 - 12x & 13 - 13x & 0 & 0 \\ \mathcal{C}_1 & 22 - 22x & 23 - 23x & 24 - 24x & 0 \\ & \mathcal{C}_2 & 33 - 33x & 34 - 34x & 35 - 35x \\ & & \mathcal{C}_3 & 44 - 44x & 45 - 45x \\ & & & & 55 - 55x \end{bmatrix} \in \mathbb{S}_+^5$$

\mathcal{C}_3
3, 4, 5
\mathcal{C}_2
3, 4
2
\mathcal{C}_1
2, 3
1

Using the transformation in (43) this constraint can be represented by three constraints on the submatrices S_1 , S_2 and S_3 and six overlap variables $\theta_1, \dots, \theta_6$:

$$S_3 = \begin{bmatrix} B_{33} - A_{33}x - \theta_1 & B_{34} - A_{34}x - \theta_2 & B_{35} - A_{35}x \\ & B_{44} - A_{44}x - \theta_3 & B_{45} - A_{45}x \\ & & B_{55} - A_{55}x \end{bmatrix} \in \mathbb{S}_+^3$$

$$S_2 = \begin{bmatrix} B_{22} - A_{22}x - \theta_4 & B_{23} - A_{23}x - \theta_5 & B_{24} - A_{24}x \\ & \theta_1 - \theta_6 & \theta_2 \\ & & \theta_3 \end{bmatrix} \in \mathbb{S}_+^3$$

$$S_1 = \begin{bmatrix} B_{11} - A_{11}x & B_{12} - A_{12}x & B_{13} - A_{13}x \\ & \theta_4 & \theta_5 \\ & & \theta_6 \end{bmatrix} \in \mathbb{S}_+^3$$

Notice how the overlap variables drop out if the original matrix S is reassembled according to Theorem 2 by adding the entries of each subblock.

5 Clique Merging

Given an initial decomposition with (chordally completed) edge set E and a set of cliques $\{\mathcal{C}_1, \dots, \mathcal{C}_p\}$, we are free to re-merge any number of cliques back into larger blocks. This is equivalent to treating *structural* zeros in the problem as *numerical* zeros, leading to additional edges in the graph. Looking at the decomposed problem in (40) and (42), the effects of merging two cliques \mathcal{C}_i and \mathcal{C}_j are twofold:

1. We replace two positive semidefinite matrix constraints of dimensions $|\mathcal{C}_i|$ and $|\mathcal{C}_j|$ with one constraint on a larger clique with dimension $|\mathcal{C}_i \cup \mathcal{C}_j|$, where the increase in dimension depends on the size of the overlap.
2. We remove consistency constraints for the overlapping entries between \mathcal{C}_i and \mathcal{C}_j , thus reducing the size of the linear system of equality constraints.

When merging cliques these two factors have to be balanced, and the optimal merging strategy depends on the particular SDP solution algorithm employed. In [NFF⁺03] and [SAV14] a clique tree is used to search for favourable merge candidates; We will refer to their two approaches as SparseCoLo and the *parent-child* strategy, respectively, in the following sections. We will then propose a new merging method in Section 5.2 whose performance is superior to both methods when used in ADMM. Given a merging strategy, Algorithm 3 describes how to merge a set of cliques within the set \mathcal{B} and update the edge set \mathcal{E} accordingly.

Algorithm 3: Function mergeCliques($\mathcal{B}, \mathcal{E}, \mathcal{B}_m$).

Input : A set of cliques \mathcal{B} with edge set \mathcal{E} , a subset of cliques $\mathcal{B}_m = \{\mathcal{C}_{m,1}, \mathcal{C}_{m,2}, \dots, \mathcal{C}_{m,r}\} \subseteq \mathcal{B}$ to be merged.

Output: A reduced set of cliques $\hat{\mathcal{B}}$ with edge set $\hat{\mathcal{E}}$ and the merged clique \mathcal{C}_m .

- 1 $\hat{\mathcal{E}} \leftarrow \mathcal{E}$;
 - 2 $\mathcal{C}_m \leftarrow \mathcal{C}_{m,1} \cup \mathcal{C}_{m,2} \cup \dots \cup \mathcal{C}_{m,r}$;
 - 3 $\hat{\mathcal{B}} \leftarrow (\mathcal{B} \setminus \mathcal{B}_m) \cup \{\mathcal{C}_m\}$;
 - 4 Remove edges $\{(\mathcal{C}_i, \mathcal{C}_j) \mid i \neq j, \mathcal{C}_i, \mathcal{C}_j \in \mathcal{B}_m\}$ in $\hat{\mathcal{E}}$;
 - 5 Replace edges $\{(\mathcal{C}_i, \mathcal{C}_j) \mid \mathcal{C}_i \in \mathcal{B}_m, \mathcal{C}_j \notin \mathcal{B}_m\}$ with $(\mathcal{C}_m, \mathcal{C}_j)$ in $\hat{\mathcal{E}}$;
-

5.1 Existing clique tree-based strategies

The parent-child strategy described in [SAV14] traverses the clique tree in a depth-first order and merges a clique \mathcal{C}_ℓ with its parent clique $\mathcal{C}_{\text{par}(\ell)} := \text{par}(\mathcal{C}_\ell)$ if at least one of the two following

conditions are met:

$$(|\mathcal{C}_{\text{par}(\ell)}| - |\eta_\ell|) (|\mathcal{C}_\ell| - |\eta_\ell|) \leq t_{\text{fill}}, \quad (47)$$

$$\max \{|\nu_\ell|, |\nu_{\text{par}(\ell)}|\} \leq t_{\text{size}}, \quad (48)$$

with heuristic parameters t_{fill} and t_{size} . These conditions keep the amount of extra fill-in and the supernode cardinalities below the specified thresholds. The `SparseCoLo` strategy described in [NFF⁺03] and [FFN06] considers parent-child as well as sibling relationships. Given a parameter $\sigma > 0$, two cliques $\mathcal{C}_i, \mathcal{C}_j$ are merged if the following merge criterion holds

$$\min \left\{ \frac{|\mathcal{C}_i \cap \mathcal{C}_j|}{|\mathcal{C}_i|}, \frac{|\mathcal{C}_i \cap \mathcal{C}_j|}{|\mathcal{C}_j|} \right\} \geq \sigma. \quad (49)$$

This approach traverses the clique tree depth-first, performing the following steps for each clique \mathcal{C}_ℓ :

1. For each clique pair $\{(\mathcal{C}_i, \mathcal{C}_j) \mid \mathcal{C}_i, \mathcal{C}_j \in \text{ch}(\mathcal{C}_\ell)\}$, check if (49) holds, then:
 - \mathcal{C}_i and \mathcal{C}_j are merged, or
 - if $(\mathcal{C}_i \cup \mathcal{C}_j) \supseteq \mathcal{C}_\ell$, then $\mathcal{C}_i, \mathcal{C}_j$, and \mathcal{C}_ℓ are merged.
2. For each clique pair $\{(\mathcal{C}_i, \mathcal{C}_\ell) \mid \mathcal{C}_i \in \text{ch}(\mathcal{C}_\ell)\}$, merge \mathcal{C}_i and \mathcal{C}_ℓ if (49) is satisfied.

We note that the open-source implementation of the `SparseCoLo` algorithm described in [NFF⁺03] follows the algorithm outlined here, but also employs a few additional heuristics.

An advantage of these two approaches is that the clique tree can be computed easily and the conditions are inexpensive to evaluate. However, a disadvantage is that choosing parameters that work well on a variety of problems and solver algorithms is difficult. Secondly, clique trees are not unique and in some cases it is beneficial to merge cliques that are not directly related on the particular clique tree that was computed. To see this, consider a chordal graph $G(V, E)$ consisting of three connected subgraphs:

$$\begin{aligned} G_a(V_a, E_a), & \text{ with } V_a = \{3, 4, \dots, m_a\}, \\ G_b(V_b, E_b), & \text{ with } V_b = \{m_a + 2, m_a + 3, \dots, m_b\}, \\ G_c(V_c, E_c), & \text{ with } V_c = \{m_b + 1, m_b + 2, \dots, m_c\}, \end{aligned}$$

and some additional vertices $\{1, 2, m_a + 1\}$. The graph is connected as shown in Figure 2(a), where the complete subgraphs are represented as nodes V_a, V_b, V_c . A corresponding clique tree is shown in Figure 2(b). By choosing the cardinality $|V_c|$, the overlap between cliques $\mathcal{C}_1 = \{1, 2\} \cup V_c$ and $\mathcal{C}_3 = \{m_a + 1\} \cup V_c$ can be made arbitrarily large while $|V_a|, |V_b|$ can be chosen so that any other merge is disadvantageous. However, neither the parent-child strategy nor `SparseCoLo` would consider merging \mathcal{C}_1 and \mathcal{C}_3 since they are in a ‘‘nephew-uncle’’ relationship. In fact for the particular sparsity graph in Figure 2(a) eight different clique trees can be computed. Only in half of them do the cliques \mathcal{C}_1 and \mathcal{C}_3 appear in a parent-child relationship. Therefore, a merge strategy that only considers parent-child relationships would miss this favorable merge in half the cases.

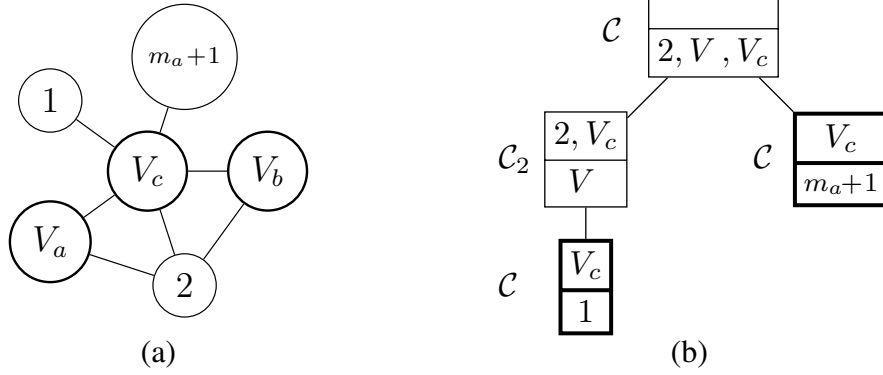


Figure 2: Sparsity graph (a) that can lead to clique tree (b) with an advantageous “nephew-uncle” merge between C_1 and C_3 .

5.2 A new clique graph-based strategy

To overcome the limitations of existing strategies we propose a merging strategy based on the *reduced clique graph* $\mathcal{G}(\mathcal{B}, \xi)$, which is defined as the union of all possible clique trees of G ; see [HS12] for a detailed discussion. The set of vertices of this graph is given by the maximal cliques of the sparsity pattern. We then create the edge set ξ by introducing edges between pairs of cliques (C_i, C_j) if they form a separating pair \mathcal{P}_{ij} . We remark that ξ is a subset of the edges present in the *clique intersection graph* which is obtained by introducing edges for every two cliques that intersect. However, the reduced clique graph has the property that it remains a valid reduced clique graph of the altered sparsity pattern after performing a permissible merge between two cliques. This is not always the case for the clique intersection graph. For convenience, we will refer to the reduced clique graph simply as the clique graph in the following sections. Based on the permissibility condition for edge reduction in [HS12] we define a permissibility condition for clique merges:

Definition 5.1 (Permissible merge).

Given a reduced clique graph $\mathcal{G}(\mathcal{B}, \xi)$, a merge between two cliques $(C_i, C_j) \in \xi$ is permissible if for every common neighbour C_k it holds that $C_i \cap C_k = C_j \cap C_k$.

We further define a monotone *edge weighting function* $e: 2^V \times 2^V \rightarrow \mathbb{R}$ that assigns a weight w_{ij} to each edge $(C_i, C_j) \in \xi$:

$$e(C_i, C_j) = w_{ij}.$$

This function is used to estimate the per-iteration computational savings of merging a pair of cliques depending on the targeted algorithm and hardware. It evaluates to a positive number if a merge reduces the per-iteration time and to a negative number otherwise. For a first-order method, whose per-iteration cost is dominated by an eigenvalue factorisation with complexity $\mathcal{O}(|C|^3)$, a simple choice would be:

$$e(C_i, C_j) = |C_i|^3 + |C_j|^3 - |C_i \cup C_j|^3. \quad (50)$$

More sophisticated weighting functions can be determined empirically; see Section 7.5. After a weight has been computed for each edge (C_i, C_j) in the clique graph, we merge cliques as outlined in Algorithm 4. This strategy considers the edges in terms of their weights, starting with the

Algorithm 4: Clique graph-based merging strategy.

Input : A weighted clique graph $\mathcal{G}(\mathcal{B}, \xi)$.

Output: A merged clique graph $\mathcal{G}(\hat{\mathcal{B}}, \hat{\xi})$.

```

1  $\hat{\mathcal{B}} \leftarrow \mathcal{B}$  and  $\hat{\xi} \leftarrow \xi$ ;
2 STOP  $\leftarrow$  false;
3 while !STOP do
4     choose permissible edge  $(C_i, C_j)$  with maximum  $w_{ij}$ ;
5     if  $w_{ij} > 0$  then
6          $\mathcal{B}_m \leftarrow \{C_i, C_j\}$ ;
7          $\hat{\mathcal{B}}, \hat{\xi}, \mathcal{C}_m \leftarrow \text{mergeCliques}(\hat{\mathcal{B}}, \hat{\xi}, \mathcal{B}_m)$ ;
8         for each edge  $(C_m, C_\ell) \in \hat{\xi}$  do
9             update  $w_{m\ell} \leftarrow e(C_m, C_\ell)$ ;
10    else
11    STOP  $\leftarrow$  true;
```

permissible clique pair (C_i, C_j) with the highest weight w_{ij} . If the weight is positive, the two cliques are merged and the edge weights for all edges connected to the merged clique $\mathcal{C}_m = C_i \cup C_j$ are updated. This process continues until no edges with positive weights remain.

The clique graph for the clique tree in Figure 1(c) is shown in Figure 3(a) with the edge weighting function in (50). Following Algorithm 4 the edge with the largest weight is considered first and the corresponding cliques are merged, i.e. $\{3, 6, 7, 8\}$ and $\{6, 7, 8, 9\}$. Note that the merge is permissible because both cliques intersect with the only common neighbour $\{4, 5, 8\}$ in the same way. The revised clique graph $\mathcal{G}(\hat{\mathcal{B}}, \hat{\xi})$ is shown in Figure 3(b). Since no edges with positive weights remain, the algorithm stops.

After Algorithm 4 has terminated, it is possible to recompute a valid clique tree from the revised clique graph. This can be done in two steps. First, the edge weights in $\mathcal{G}(\hat{\mathcal{B}}, \hat{\xi})$ are replaced with the cardinality of their intersection:

$$\tilde{w}_{ij} = |C_i \cap C_j|, \text{ for all } (C_i, C_j) \in \hat{\xi}.$$

Second, a clique tree is then given by any *maximum weight spanning tree* of the newly weighted clique graph, e.g. using Kruskal’s algorithm described in [Kru56].

Our merging strategy has some clear advantages over competing approaches. Since the clique graph covers a wider range of merge candidates, it will consider edges that do not appear in clique tree-based approaches such as the “nephew-uncle” example in Figure 2. Moreover, the edge

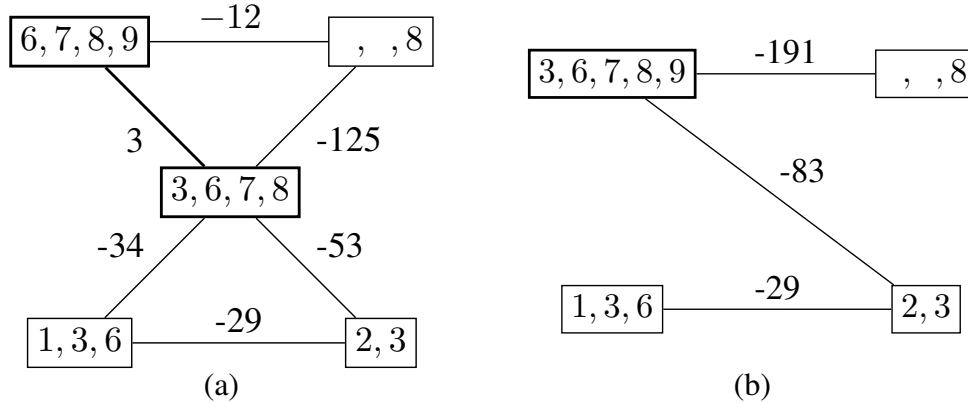


Figure 3: (a) Clique graph $\mathcal{G}(\mathcal{B}, \xi)$ of the clique tree in Figure 1(c) with edge weighting function $e(\mathcal{C}_i, \mathcal{C}_j) = |\mathcal{C}_i|^3 + |\mathcal{C}_j|^3 - |\mathcal{C}_i \cup \mathcal{C}_j|^3$ and (b) clique graph $\mathcal{G}(\hat{\mathcal{B}}, \hat{\xi})$ after merging the cliques $\{3, 6, 7, 8\}$ and $\{6, 7, 8, 9\}$ and updating edge weights.

weighting function allows one to make a merge decision based on the particular solver algorithm and hardware used. One downside is that this approach is more computationally expensive than the other methods. However, our numerical experiments show that the time spent on finding the clique graph, merging the cliques, and recomputing the clique tree represent only a very small fraction of the total computational savings relative to other merging methods when solving SDPs.

6 Open-Source Implementation

We have implemented our algorithm in the Conic Operator Splitting Method (COSMO), an open-source package written in Julia [BEKS17]. Julia allows the solver to be written in a flexible, modular and extensible way, while still maintaining the benefits of a fast compiled language. The source code and documentation are available at

<https://github.com/oxfordcontrol/COSMO.jl>.

COSMO offers the user two interfaces to describe the constraints of the optimisation problem: a direct interface, and an interface to the modelling languages JuMP [DHL17] and Convex.jl [UMZ⁺14]. These interfaces connect the solver to the Julia optimisation ecosystem which provide flexible problem description and automatic problem reformulation.

As shown in Algorithm 1 the two main steps of the algorithm are solving a linear system and projecting onto a Cartesian product of cones. The implementation of these two parts allows customisation by the user. For the solution of the linear system in (17) the user can either use the QDLDL [SBG⁺18] solver provided with COSMO, the standard sparse solver from SuiteSparse [D⁺15], or choose one of the provided interfaces to direct and indirect solvers, e.g. Pardiso [SGK⁺10, KAA⁺15], conjugate gradient, minimal residual method, or link their own implementation.

The second important part of the algorithm is the projection step onto a Cartesian product of convex sets. By default `COSMO` supports the zero cone, the nonnegative orthant, the hyperbox, the second-order cone, the PSD cone, the exponential cone and its dual, and the power cone and its dual. Our Julia implementation also allows the user to define their own convex cones² and custom projection functions. To implement a custom cone \mathcal{K}_c the user has to provide:

- a projection function that projects an input vector onto the cone
- a function that determines if a vector is inside the dual cone \mathcal{K}_c^*
- a function that determines if a vector is inside the recession cone of $-\mathcal{K}_c$

The latter two functions are required for our solver to implement checks for infeasibility as described in Sections 2.1 and 3.4. An example that shows the advantages of defining a custom cone is provided in Section 7.2.

The authors in [RGN19] used `COSMO`'s algorithm with a specialized implementation of the projection function for positive semidefinite constraints. The projection method used approximate matrix eigendecompositions to significantly reduce the projection time, while maintaining all the features of `COSMO` such as scaling, infeasibility detection and interfaces to linear system solvers. It was demonstrated that this can provide a significant, up to 20x, reduction in solve time.

Given a problem with multiple constraints, the projection step (19) can be carried out in parallel. This is particularly advantageous when used in combination with chordal decomposition, which typically yields a large number of smaller PSD constraints. For the eigendecomposition involved in the projection step of a PSD constraint, the LAPACK [ABB⁺99] function `sveyr` is used, which can also utilise multiple threads. Consequently, this leads to two-level parallelism in the computation, i.e on the higher level the projection functions are carried out in parallel and each projection function independently calls `sveyr`. Determining the optimal allocation of the CPU cores to each of these tasks depends on the number of PSD constraints and their dimensions and is a difficult problem. For the problem sets considered in section 7 we achieved the best performance by running `sveyr` single-threaded and using all physical CPUs to carry out the projection functions in parallel.

Moreover, Julia's type abstraction features are used to enable the solver to solve problems of arbitrary floating-point precision. This allows for example to reduce the memory usage of the solver for very large problems by switching to 32-bit single-precision floating-point format.

²To allow infeasibility detection the user has to either define a convex cone, a convex compact set or a composition of the two.

7 Numerical Results

This section presents benchmark results of COSMO against the interior-point solver MOSEK v9.0 and the accelerated first-order ADMM solver SCS v2.1.1. When applied to a quadratic program, COSMO’s main algorithm becomes very similar to the first-order QP solver OSQP. To test the performance penalty of using a pure Julia implementation against a similar C implementation we also compare our solver against OSQP v0.6.0 on QP problems.

We selected a number of problem sets to test different aspects of COSMO. The advantage of supporting a quadratic cost function in a conic solver is shown by solving QPs from the Maros and Mészáros QP repository [MM99] in Section 7.1 and SDPs with quadratic objectives in the form of nearest correlation matrix problems in Section 7.3.

To highlight the advantages of implementing custom constraints, we consider a problem set with doubly-stochastic matrices in Section 7.2. We then show how chordal decomposition can speed up the solver for SDPs that exhibit a block-arrow sparsity pattern in Section 7.4.

The performance of chordal decomposition is further explored in Section 7.5 by solving large structured problems from the SDPLib benchmark set [Bor99] as well as some non-chordal SDPs generated with sparsity patterns from the SuiteSparse Matrix Collections [DH11]. Using the same problems we additionally evaluate the performance of different clique merging strategies.

All the experiments were carried out on a computing node of the University of Oxford ARC-HTC cluster with 16 logical Intel Xeon E5-2560 cores and 64 GB of DDR3 RAM. All the problems were run using Julia v1.3 and the problems were passed to the solvers via MathOptInterface [LDGL20].

To evaluate the accuracy of the returned solution we compute three errors adapted from the DIMACS error measures for SDPs [JPA00]:

$$\epsilon_1 = \frac{\|A_a x - b_a\|_2}{1 + \|b_a\|_2}, \quad \epsilon_2 = \frac{\|Px + q - A_a^\top y_a\|_2}{1 + \|q\|_2}, \quad \epsilon_3 = \frac{|x^\top Px + q^\top x - b_a^\top y_a|}{1 + |q^\top x| + |b_a^\top y_a|}, \quad (51)$$

where A_a , b_a and y_a correspond to the rows of A , b and y that represent active constraints. This is to ensure meaningful values even if the problem contains inactive constraints with very large, or possibly infinite, values b_i . The maximum of the three errors for each problem and solver is reported in the results below.

We configured COSMO, MOSEK, SCS and OSQP to achieve an accuracy of $\epsilon = 10^{-3}$. We set the maximum allowable solve time for the Maros and Mészáros problems to 5 min and to 30 min for the other problem sets. All other solver parameters were set to the solvers’ standard configurations. COSMO uses a Julia implementation of the QDLDL solver to factor the quasi-definite linear system. Similarly, we configured SCS to use a direct solver for the linear system.

7.1 Maros and Mészáros QP test set

The Maros and Mészáros test problem set [MM99] is a repository of challenging convex QP problems that is widely used to compare the performance of QP solvers. For comparison metrics we compute the failure rate, the number of fastest solve time and the normalized shifted geometric mean for each solver. The shifted geometric mean is more robust against large outliers (compared to the arithmetic mean) and against small outliers (compared to the geometric mean) and is commonly used in optimisation benchmarks; see [SBG⁺18, Mit]. The shifted geometric mean $\mu_{g,s}$ is defined as:

$$\mu_{g,s} := \sqrt[n]{\prod_p (t_{p,s} + sh)} - sh \quad (52)$$

with total solver time $t_{p,s}$ of solver s and problem p , shifting factor sh and size of the problem set n . In the reported results a shifting factor of $sh = 10$ was chosen and the maximum allowable time $t_{p,s} = 300$ s was used if solver s failed on problem p . Lastly, we normalize the shifted geometric mean for solver s by dividing by the geometric mean of the fastest solver. The failure rate $f_{r,s}$ is given by the number of unsolved problems compared to the total number of problems in the problem set. As unsolved problems we count instances where the algorithm does not converge within the allowable time or fails during the setup or solve phase. Table 1 shows the normalized shifted geometric mean and the failure rate for each solver. Additionally, the number of cases where solver s was the fastest solver is shown.

Table 1: Normalized shifted geometric mean and failure rates for solvers tested on the Maros and Mészáros QP test set.

	OSQP	COSMO	MOSEK	SCS
Normalized shifted geometric mean	1.000	1.169	1.897	75.015
Number of fastest solve time	75	27	33	0
Failure rates $f_{r,s}$ [%]	4.444	5.185	10.370	83.704

OSQP shows the best performance in terms of lowest failure rates, number of fastest solves and in the shifted geometric mean of solve times. COSMO follows very closely. The shifted geometric mean of MOSEK seems to suffer from a higher failure rate compared to OSQP/COSMO, and SCS fails on a large number of problems. The higher failure rate could be due to the necessary transformation into a second-order-cone problem.

For this problem set of QPs COSMO’s algorithm reduces, with some minor differences, to the algorithm of OSQP. Consequently, this benchmark is useful to evaluate the performance penalty that COSMO pays due to its implementation in the higher-order language Julia. The results in Table 1 show that the performance difference is very small. This can also be seen by looking at the solve times of each solver for increasing problem dimension, as shown in Figure 4.

COSMO and OSQP have very similar solve times, aside from very small problems that are solved in under 1×10^{-5} s to 1×10^{-4} s. This difference is primarily due to overheads incurred from

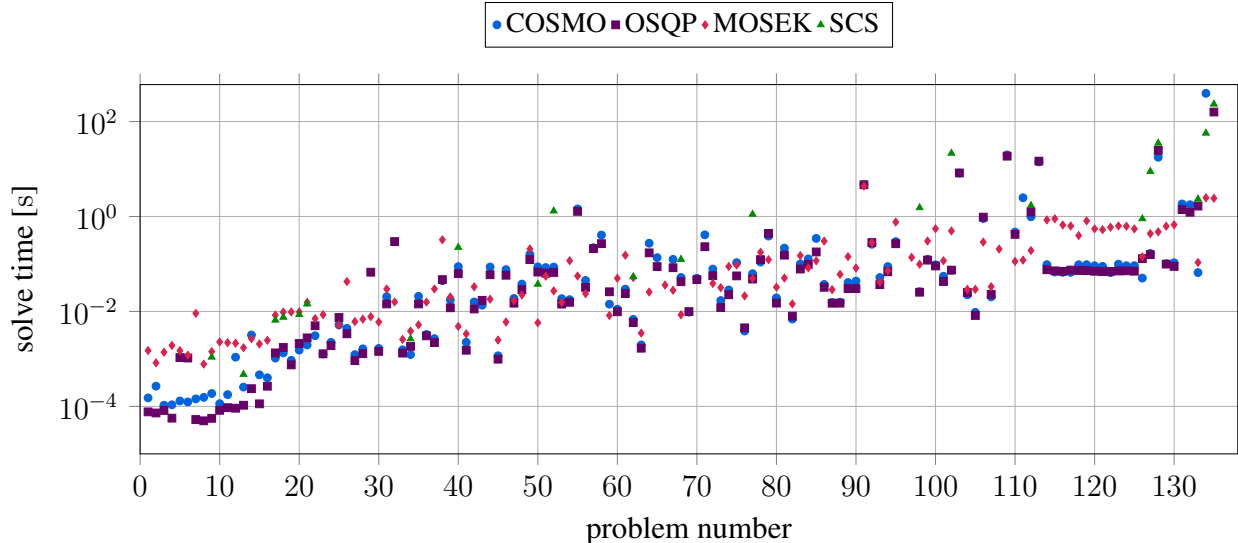


Figure 4: Solve time of benchmarked solvers for problems of the Maros and Mészáros QP problem set. Only problem results classified as solved are shown. The problems are ordered by increasing number of non-zeros in the constraint matrix.

features in our Julia implementation that support more than one constraint type during problem setup. The marginally better resulting performance of OSQP for the smallest problems in the test set is the reason that OSQP is the faster solver in a larger number of cases in Table 1.

7.2 Custom convex cones

In many cases writing a custom solver algorithm for a particular problem can be faster than using available solver packages if a particular aspect of the problem structure can be exploited to speed up parts of the computations. As mentioned earlier, COSMO supports user customisation by allowing the definition of new convex cones. This is useful if constraints of the problem can be expressed using this new convex cone and a fast projection method onto the cone exists. A fast specialized projection method in an ADMM framework has for example been used by the authors in [BLDR13] to solve the error-correcting code decoding problem.

To demonstrate the advantage of custom convex cones, consider the problem of finding the doubly stochastic matrix that is nearest, in the Frobenius norm, to a given symmetric matrix $C \in \mathbb{S}^n$. Doubly stochastic matrices are used for instance in spectral clustering [ZS07] and matrix balancing [RHD⁺14]. A specialized algorithm for this problem type has been recently discussed by the authors in [RG19]. Doubly stochastic matrices have the property that all rows and columns each sum to one and all entries are nonnegative. The nearest doubly stochastic matrix X can be found

by solving the following optimisation problem:

$$\begin{aligned}
& \text{minimize} && \frac{1}{2} \|X - C\|_F^2 \\
& \text{subject to} && X_{ij} \geq 0 \\
& && X\mathbf{1} = \mathbf{1} \\
& && X^\top \mathbf{1} = \mathbf{1},
\end{aligned} \tag{53}$$

with symmetric real matrix $C \in \mathbb{S}^n$ and decision variable $X \in \mathbb{R}^{n \times n}$. This problem can be solved as a QP in the following form using equality and inequality constraints:

$$\begin{aligned}
& \text{minimize} && \frac{1}{2}(x^\top x - 2c^\top x + c^\top c) \\
& \text{subject to} && \begin{bmatrix} \mathbf{1}_n^\top \otimes I_n \\ I_n \otimes \mathbf{1}_n^\top \\ -I_{n^2} \end{bmatrix} x + s = \begin{bmatrix} \mathbf{1}_{2n} \\ \mathbf{1}_{2n} \\ \mathbf{0}_{n^2} \end{bmatrix} \\
& && s \in \{0\}^{4n} \times \mathbb{R}_+^{n^2},
\end{aligned} \tag{54}$$

with $x = \text{vec}(X)$ and $c = \text{vec}(C)$. However, the problem can be written in a more compact form by using a custom projection function to project the matrix iterate onto the affine set of matrices \mathcal{C}_Σ , whose rows and columns each sum to one. In general the projection of vector $s \in \mathbb{R}^n$ onto the affine set $\mathcal{C}_a = \{s \in \mathbb{R}^n \mid As = b\}$ is given by:

$$\Pi_{\mathcal{C}_a}(s) = s - A^\top (AA^\top)^{-1} (As - b), \tag{55}$$

where A is assumed to have full rank. In the case of $\mathcal{C}_a = \mathcal{C}_\Sigma$ we can exploit the fact that the inverse of AA^\top can be efficiently computed. The projection can be carried out as described in Algorithm 5; see Appendix B.1 for a derivation. Notice that Algorithm 5 can be implemented efficiently without

Algorithm 5: Projection of $s \in \mathbb{R}^n$ onto \mathcal{C}_Σ

- 1 $A_r = \mathbf{1}_n^\top \otimes I_n \quad A_c = [I_{n-1} \otimes \mathbf{1}_n^\top \quad \mathbf{0}_{(n-1) \times n}]$;
 - 2 $A = [A_r \quad A_c]^\top$;
 - 3 $r = [r_1, r_2]^\top = As - \mathbf{1}_{2n-1}$;
 - 4 $\eta_2 = \frac{1}{n} (I_{n-1} + \mathbf{1}_{n-1} \mathbf{1}_{n-1}^\top) \cdot (r_2 - \frac{1}{n} \mathbf{1}_{n-1} \mathbf{1}_{n-1}^\top r_1)$;
 - 5 $\eta_1 = \frac{1}{n} (r_1 - \mathbf{1}_n \mathbf{1}_{n-1}^\top \eta_2)$;
 - 6 $\eta = [\eta_1, \eta_2]^\top$;
 - 7 $\Pi_{\mathcal{C}_\Sigma}(s) = s - A^\top \eta$;
-

ever assembling and storing A and $\mathbf{1}\mathbf{1}^\top$. By using the custom convex set \mathcal{C}_Σ and the corresponding projection function, (53) can now be rewritten as:

$$\begin{aligned}
& \text{minimize} && (1/2)(x^\top x - 2c^\top x + c^\top c) \\
& \text{subject to} && \begin{bmatrix} -I_{n^2} \\ -I_{n^2} \end{bmatrix} x + s = \mathbf{0}_{2n^2} \\
& && s \in \mathcal{C}_\Sigma \times \mathbb{R}_+^{n^2}.
\end{aligned} \tag{56}$$

The sparsity pattern of the new constraint matrix A only consists of two diagonals and the number of non-zeros reduces from $3n^2$ to $2n^2$. We expect this to reduce the initial factorisation time of the linear system in (17) as well as the forward- and back-substitution steps.

Figure 5 shows the total solve time of all the solvers for problem (53) with randomly generated dense matrix C with $C_{ij} \sim \mathcal{U}(0, 1)$ and increasing matrix dimension. Additionally, we show the solve time for COSMO in the problem form (53) and with a specialized custom set and projection function as in (56). It is not surprising that COSMO and OSQP scale in the same way for this prob-

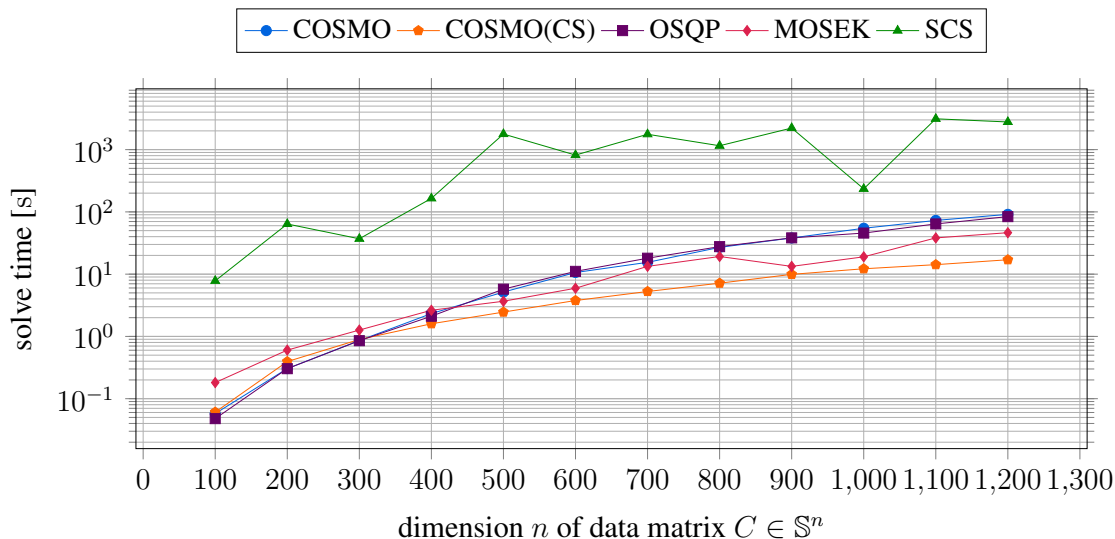


Figure 5: Solve time of benchmarked solvers for increasing problem size of doubly stochastic matrix problems. The orange line shows the solve time of COSMO (CS) with a custom convex set and projection function.

lem type. MOSEK is slightly slower for smaller problem dimension and overtakes COSMO/OSQP for problems of dimensions $n \geq 500$. This might be due to fact that MOSEK uses a faster multi-threaded linear system solver while OSQP/COSMO rely on the single-threaded solver QDLDL. The longer solve time of SCS is due to slow convergence of the algorithm for this problem type. Furthermore, when the problem is solved with a custom convex set as in (56) COSMO(CS) is able to outperform all other solvers. Table 2 shows the total solve time and the factorisation time of the two versions of COSMO for small, medium and large problems. As predicted the lower solve time can be mainly attributed to the faster factorisation time.

7.3 Nearest correlation matrix

Consider the problem of projecting a matrix C onto the set of correlation matrices, i.e. real symmetric positive semidefinite matrices with diagonal elements equal to 1. This problem is for example relevant in portfolio optimisation [Hig02]. The correlation matrix of a stock portfolio might lose

Table 2: Solve times and factorisation times of COSMO and COSMO (CS) for small, medium and large doubly stochastic matrix problems.

n	Factorisation time (s)		Solve time (s)	
	COSMO	COSMO(CS) ¹	COSMO	COSMO(CS) ¹
100	0.018	0.006	0.058	0.061
400	0.995	0.138	2.329	1.596
800	13.551	0.552	26.932	7.163
1200	52.717	1.322	91.278	17.032

¹ solving (56) with a custom convex set \mathcal{C}_Σ and projection function

its positive semidefiniteness due to noise and rounding errors of previous data manipulations. Consequently, it is of interest to find the nearest correlation matrix X to a given data matrix $C \in \mathbb{R}^{n \times n}$. The problem is given by:

$$\begin{aligned}
 & \text{minimize} && \frac{1}{2} \|X - C\|_F^2 \\
 & \text{subject to} && X_{ii} = 1, \quad i = 1, \dots, n \\
 & && X \in \mathbb{S}_+^n.
 \end{aligned} \tag{57}$$

In order to transform the problem into the standard form (3) used by COSMO, C and X are vectorized and the objective function is expanded:

$$\begin{aligned}
 & \text{minimize} && (1/2)(x^\top x - 2c^\top x + c^\top c) \\
 & \text{subject to} && \begin{bmatrix} E \\ -I \end{bmatrix} x + s = \begin{bmatrix} \mathbf{1}_n \\ \mathbf{0}_{n^2} \end{bmatrix} \\
 & && s \in \{0\}^n \times \mathcal{S}_+^n,
 \end{aligned} \tag{58}$$

with $c = \text{vec}(C) \in \mathbb{R}^{n^2}$ and $x = \text{vec}(X) \in \mathbb{R}^{n^2}$. Here $E \in \mathbb{R}^{n \times n^2}$ is a matrix that extracts the n diagonal entries X_{ii} from its vectorized form x .

For the benchmark problems we randomly sample the data matrix C with entries $C_{i,j} \sim \mathcal{U}(-1, 1)$ from a uniform distribution. Figure 6 shows the benchmark results for increasing matrix dimension n . Unsurprisingly, the first-order methods SCS and COSMO outperform the interior-point solver MOSEK for these large SDPs. Furthermore, for larger problems the solve times of COSMO and SCS scale in a similar way. COSMO seems to benefit from directly supporting the quadratic objective term in the problem while SCS has to transform it into an additional second-order-cone constraint. This increases the factorisation time and the projection time; see Table 5.

7.4 Block-arrow sparse SDPs

To demonstrate the benefits of the chordal decomposition discussed in Section 4, we consider randomly generated SDPs of the form (36) with a block-arrow aggregate sparsity pattern similar to

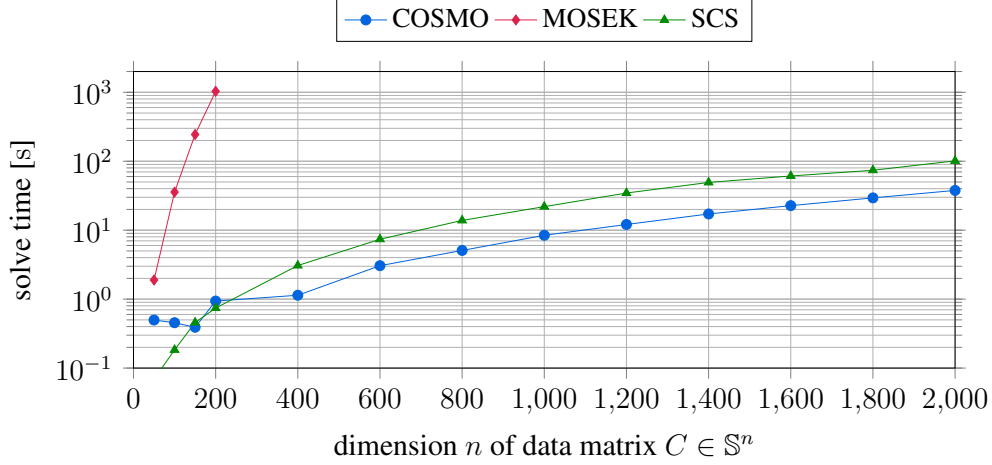


Figure 6: Solve time of benchmarked solvers for increasing problem size of nearest correlation matrix problems. The results for MOSEK are shown until they exceeded the time limit of 30 min.

test problems in [ZFP⁺19, ADV10]. Figure 7 shows the sparsity pattern of the PSD constraint. The sparsity pattern is generated based on the following parameters: block size d , number of blocks N_b and width of the arrow head w . Note that the graph corresponding to the sparsity pattern is always chordal and that, for this sparsity pattern, clique merging yields no benefit. In the following we

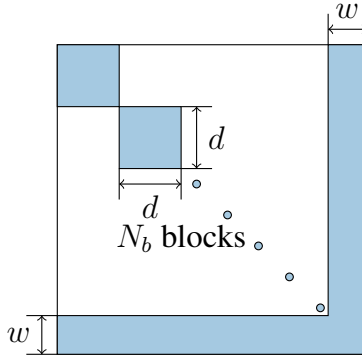


Figure 7: Parameters of block-arrow sparsity pattern. The shaded area represents the non-zeros of the sparsity pattern.

study the effects of independently increasing the block size d and the number of blocks N_b . The parameters for the two test cases are:

- Varying the number of blocks: $N_b = 50, 60, \dots, 140$, $d = 10$, $w = 20$, and $m = 100$.
- Varying the block size: $d = 10, 12, \dots, 28$, $N_b = 50$, $w = 10$, and $m = 100$.

The solve times for all solvers are shown in Figure 8, Figure 9 and in Table 6. The line COSMO (CD) corresponds to the solver with chordal decomposition enabled.

The figures show that both COSMO with and without chordal decomposition solve this problem type

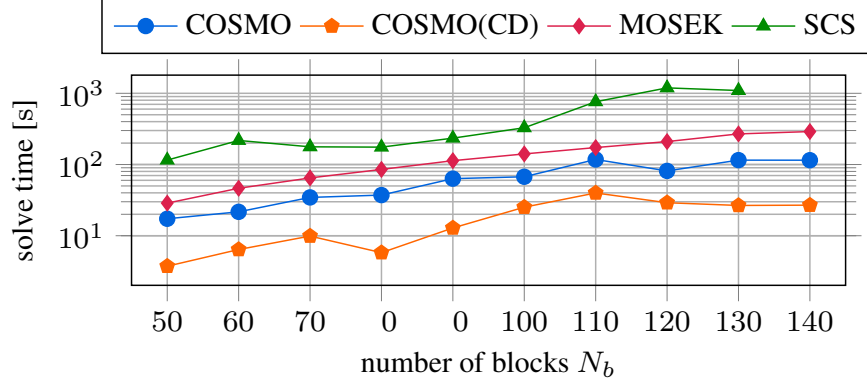


Figure 8: Solve time for increasing number of blocks N_b of block-arrow sparsity pattern.

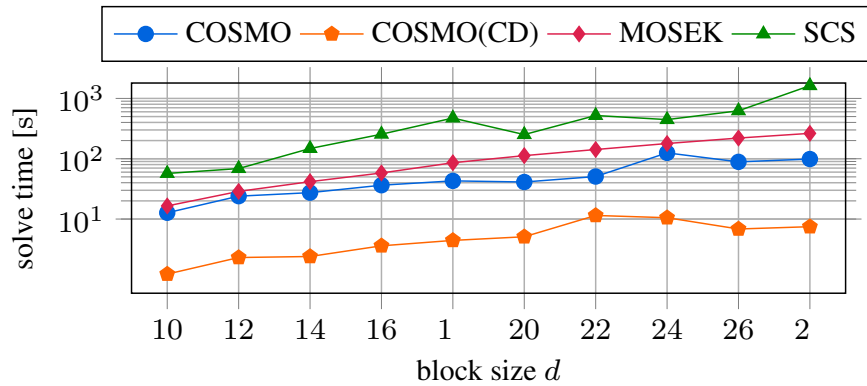


Figure 9: Solve time for increasing block size d of block-arrow sparsity pattern.

consistently faster than MOSEK and SCS. The reason why COSMO performs better than the other first order solver SCS can be explained by the significantly lower number of iterations (Table 6). Furthermore, one can see that in both cases the solver time for each solver rises when the number of blocks and the block sizes are increased. The increase is smaller for COSMO (CD) which is more affected by the number of iterations than the problem dimension.

7.5 Non-chordal problems with clique merging

To compare our proposed clique graph-based merge approach with the clique tree-based strategies of [NFF⁺03] and [SAV14], all three methods discussed in Section 5 were used to preprocess large sparse SDPs from SDPLib, a collection of SDP benchmark problems [Bor99]. This problem set contains maximum cut problems, SDP relaxations of quadratic programs and Lovász theta problems. Moreover, we consider a set of test SDPs generated from (non-chordal) sparsity patterns of matrices from the SuiteSparse Matrix Collections [DH11]. The sparsity patterns for these problems are shown in Figure 10.

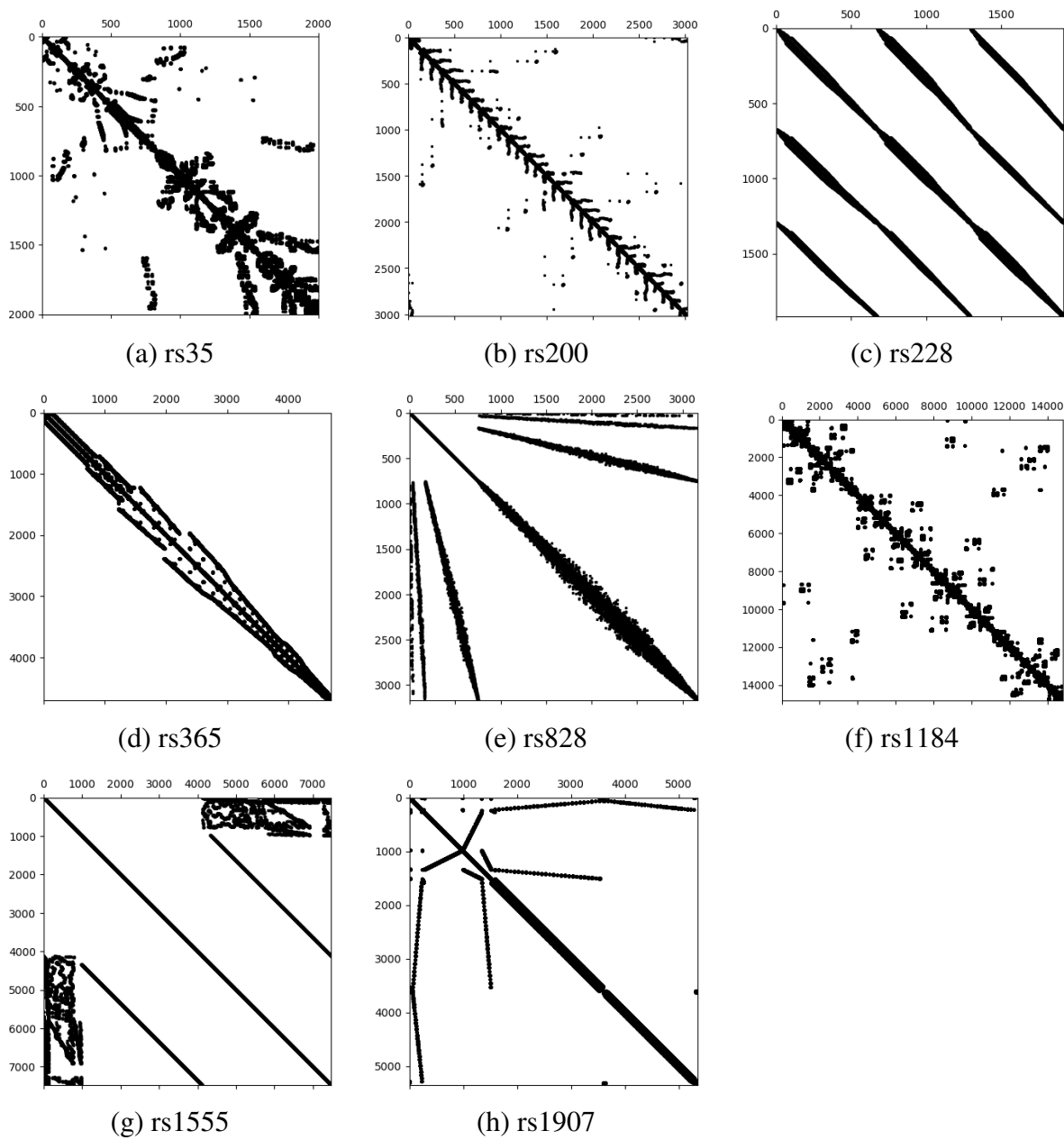


Figure 10: Aggregate sparsity pattern of non-chordal SDPs created from matrices of the SuiteSparse Matrix Collection. The patterns are labeled with their ID number.

Both problem sets were used in the past to benchmark structured SDPs [ZFP⁺19, ADV10]. This section discusses how the different decompositions affect the per-iteration computation times of the solver. In a second step we compare the solver time of COSMO with our clique graph merging strategy to those of MOSEK and SCS.

For the strategy described in [NFF⁺03] we used the SparseCoLo package to decompose the problem. The parent-child method discussed in [SAV14] and the clique graph based method described in Section 5.2 are available as options in COSMO. We further investigate the effect of using different edge weighting functions. The major operation affecting the per-iteration time is the projection step. This step involves an eigenvalue decomposition of the matrices corresponding to the cliques. Since the eigenvalue decomposition of a symmetric matrix of dimension N has a complexity of $\mathcal{O}(N^3)$, we define a *nominal* edge weighting function as in (50). However, the exact relationship will be different because the projection function involves copying of data and is affected by hardware properties such as cache size. We therefore also consider an empirically *estimated* edge weighting function. To determine the relationship between matrix size and projection time, the execution time of the relevant function inside COSMO was measured for different matrix sizes. We then approximated the relationship between projection time, t_{proj} , and matrix size, N , as a polynomial:

$$t_{\text{proj}}(N) = aN^3 + bN^2,$$

where a, b were estimated using least squares (Figure 11). The estimated weighting function is then defined as

$$e(\mathcal{C}_i, \mathcal{C}_j) = t_{\text{proj}}(|\mathcal{C}_i|) + t_{\text{proj}}(|\mathcal{C}_j|) - t_{\text{proj}}(|\mathcal{C}_i \cup \mathcal{C}_j|). \quad (59)$$

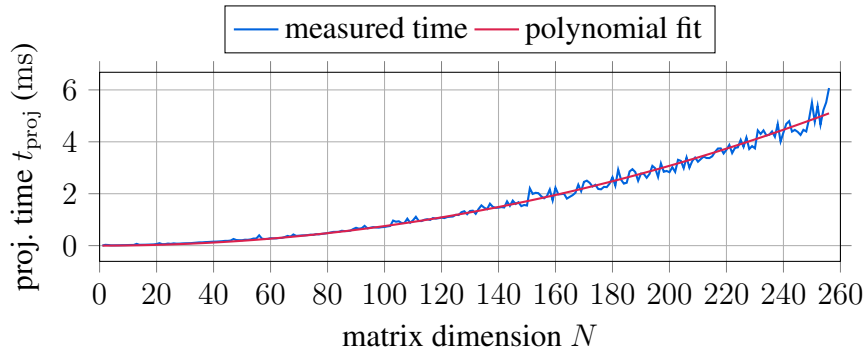


Figure 11: Measured and estimated relationship between matrix size and execution time of the projection function in COSMO.

Six different cases were considered: no decomposition (NoDe), no clique merging (NoMer), decomposition using SparseCoLo (SpCo), parent-child merging (ParCh), and the clique graph-based method with nominal edge weighting (CG1) and estimated edge weighting (CG2). SparseCoLo was used with default parameters. All cases were run single-threaded. Since the per-iteration projection times for some problems lie in the millisecond range every problem was benchmarked ten times and the median values are reported. Table 3 shows the solve time, the mean projection time, the number of iterations, the number of cliques after merging, and the maximum clique size of the

sparsity pattern for each problem and strategy. The solve time includes the time spent on decomposition and clique merging. We do not report the total solver time when `SparseCoLo` was used for the decomposition because this has to be done in a separate preprocessing step in `MATLAB` which was orders of magnitude slower than the other methods.

Our clique graph-based methods lead to a reduction in overall solver time. The method with estimated edge weighting function `CG2` achieves the lowest average projection times for the majority of problems. In four cases `ParCh` has a narrow advantage. The geometric mean of the ratios of projection time of `CG2` compared to the best non-graph method is 0.701, with a minimum ratio of 0.407 for problem `mcp500-2`. There does not seem to be a clear pattern that relates the projection time to the number of cliques or the maximum clique size of the decomposition. This is expected as the optimal merging strategy depends on the properties of the initial decomposition such as the overlap between the cliques. The merging strategies `ParCh`, `CG1` and `CG2` generally result in similar maximum clique sizes compared to `SparseCoLo`, with `CG1` being the most conservative in the number of merges.

Table 4 shows the benchmark results of `COSMO` with merging strategy `CG2`, `MOSEK`, and `SCS`. The decomposition helps `COSMO` to solve most problems faster than `MOSEK` and `SCS`. This is even more significant for the larger problems that were generated from the `SuiteSparse Matrix Collection`. The decomposition does not seem to provide a major benefit for the slightly denser problems `mcp500-3` and `mcp500-4`. Furthermore, `COSMO` seems to converge slowly for `qpG51` and `thetaG51`. Similar observations for `mcp500-3`, `mcp500-4` and `thetaG51` have been made by the authors in [ADV10]. Finally, many of the larger problems were not solvable within the time limit or caused out-of-memory problems if no decomposition was used in `MOSEK` and `SCS`.

8 Conclusions

This paper describes the first-order solver `COSMO` and the `ADMM` algorithm on which it is based. The solver combines direct support of quadratic objectives, infeasibility detection, custom constraints, chordal decomposition of `PSD` constraints and automatic clique merging. The performance of the solver is illustrated on a number of benchmark problems that challenge different aspects of modern solvers.

The implementation in the `Julia` language facilitates rapid development and testing of ideas and allows users to customize the solver for their applications. It further allows the abstraction of precision and array types which we are planning to use to allow `COSMO` to run on `GPUs`. Further performance gains are likely to be achieved by exploring acceleration methods to speed up convergence to higher accuracies and reduce the dependency on problem scaling.

A Appendix

A.1 Benchmark Results

Table 3: Benchmark results for non-chordal sparse SDPs from SDPLib and SDPs generated with sparsity patterns from the SuiteSparse Matrix Collection for different merging strategies.

problem	Median Solve time (s)						Median Projection time (ms)					
	NoDe ¹	NoMer ²	SpCo ³	ParCh ⁴	CG1 ⁵	CG2 ⁶	NoDe	NoMer	SpCo	ParCh	CG1	CG2
maxG11	35.85	4.69	***	3.33	3.09	2.93	143.3	18.4	12.7	10.5	13.4	11.2
maxG32	407.82	25.95	***	15.62	14.38	19.56	1257.7	73.2	73.1	49.9	51.6	43.1
maxG51	40.61	32.8	***	9.56	6.93	9.62	245.8	230.4	219.3	122.2	65.5	58.5
mcp500-1	21.46	1.33	***	0.7	0.89	0.6	56.0	7.7	7.4	4.6	6.1	4.9
mcp500-2	13.55	12.28	***	8.37	2.6	2.42	54.9	45.4	32.1	28.0	14.3	11.4
mcp500-3	11.28	32.45	***	30.13	7.01	5.14	51.1	104.9	105.0	83.4	28.2	21.2
mcp500-4	14.57	72.27	***	13.87	5.84	7.67	59.2	253.8	193.8	141.2	44.1	35.8
qpG11	142.31	7.3	***	4.79	4.62	4.7	305.1	20.0	12.3	10.9	15.6	13.2
qpG51	450.74	186.49	***	89.81	150.86	132.68	523.6	247.2	246.9	134.1	73.9	65.2
thetaG11	332.06	9.43	***	9.43	9.46	6.81	477.5	21.9	18.9	12.5	16.3	14.5
thetaG51	1062.91	110.64	***	107.02	37.22	85.92	252.8	230.8	** * [†]	131.7	66.5	53.7
rs1184	** * ^m	1227.48	***	882.27	632.96	569.29	** * ^m	4192.8	3495.8	3424.1	2483.9	2301.3
rs1555	** * [†]	79.83	***	65.93	80.72	83.84	** * [†]	316.7	242.7	268.8	160.7	132.1
rs1907	** * [†]	233.86	***	197.99	178.79	166.23	** * [†]	483.8	490.3	455.3	382.7	352.1
rs200	640.0	31.33	***	21.09	24.78	19.29	3366.2	121.6	93.0	82.9	93.2	71.7
rs228	206.2	40.88	***	27.79	25.29	18.6	1220.2	116.0	59.4	76.2	67.1	50.9
rs35	296.52	196.93	** *	146.56	88.86	71.25	1269.8	548.1	358.2	404.6	272.5	223.2
rs365	** * [†]	159.75	***	127.77	110.48	92.5	** * [†]	433.1	364.6	351.1	289.9	262.0
rs828	603.55	29.86	***	19.24	23.25	17.81	3716.7	113.2	80.0	71.1	87.5	64.2

problem	Iterations						Number of cliques / Maximum clique size					
	NoDe	NoMer	SpCo	ParCh	CG1	CG2	NoDe	NoMer	SpCo	ParCh	CG1	CG2
maxG11	225	225	500	275	200	225	1/800	598/24	13/80	198/32	473/28	407/36
maxG32	300	300	425	250	225	375	1/2000	1498/76	21/210	481/76	1164/92	664/102
maxG51	150	100	75	50	75	125	1/1000	674/326	181/322	163/326	448/362	313/395
mcp500-1	350	150	150	125	125	100	1/500	457/39	451/44	105/43	437/54	361/65
mcp500-2	225	225	200	250	150	175	1/500	363/138	144/138	96/140	316/156	226/171
mcp500-3	200	250	250	300	200	200	1/500	259/242	101/242	71/242	211/263	135/285
mcp500-4	225	225	375	75	100	175	1/500	161/340	63/346	46/341	105/368	87/393
qpG11	400	325	525	375	250	300	1/1600	1398/24	813/80	287/32	1273/28	1207/36
qpG51	750	600	800	550	1800	1825	1/2000	1674/326	1182/304	275/326	1448/362	1313/395
thetaG11	675	375	2275	650	500	400	1/801	598/25	13/81	198/33	494/29	423/41
thetaG51	3825	325	** * [†]	575	375	1250	1/1001	676/324	150/323	157/324	424/358	267/396
rs1184	** * ^m	225	200	200	200	200	1/14822	2236/500	78/1330	1043/500	664/608	258/632
rs1555	** * [†]	150	150	150	150	175	1/7479	6891/184	3350/187	2556/184	5529/236	4858/276
rs1907	** * [†]	200	200	175	175	200	1/5357	577/261	47/585	419/261	441/324	219/405
rs200	175	125	125	125	125	125	1/3025	1632/95	94/216	444/95	1123/112	583/119
rs228	150	125	125	125	125	125	1/1919	790/88	48/180	255/88	369/95	129/127
rs35	200	175	200	175	150	150	1/2003	589/343	53/735	189/343	214/457	106/520
rs365	** * [†]	175	175	175	175	175	1/4704	1230/296	110/350	539/296	688/349	346/474
rs828	150	125	150	125	125	125	1/3169	1875/86	112/174	501/86	1378/102	708/126

[†] time limit reached; ^m out of memory error; ¹ no decomposition; ² no merging; ³ SparseCoLo merging;
⁴ parent-child merging; ⁵ clique graph with nominal edge weighting (50);
⁶ clique graph with estimated edge weighting (59);

Table 4: Benchmark results for non-chordal sparse SDPs from SDPLib and SDPs generated with sparsity patterns from the SuiteSparse Matrix Collection.

problem	Solve time (s)			Iterations			Max error ²		
	COSMO ¹	MOSEK	SCS	COSMO ¹	Mosek	SCS	COSMO ¹	MOSEK	SCS
maxG11	1.47	4.45	131.8	225	5	1220	7.84×10^{-4}	1.98×10^{-3}	8.74×10^{-4}
maxG32	6.25	50.84	840.79	375	5	1220	9.74×10^{-4}	2.76×10^{-3}	6.87×10^{-4}
maxG51	8.09	9.92	36.56	125	8	180	2.31×10^{-3}	2.83×10^{-4}	8.85×10^{-4}
mcp500-1	0.24	1.7	29.28	100	7	580	1.02×10^{-3}	1.52×10^{-3}	6.31×10^{-4}
mcp500-2	1.68	1.75	17.36	175	7	380	6.82×10^{-4}	7.37×10^{-4}	3.30×10^{-4}
mcp500-3	4.41	1.68	8.36	200	6	180	2.23×10^{-3}	4.18×10^{-4}	6.86×10^{-4}
mcp500-4	8.2	1.76	7.4	175	7	160	1.65×10^{-3}	2.79×10^{-4}	3.43×10^{-4}
qpG11	2.36	26.23	734.7	300	7	1820	4.57×10^{-4}	1.28×10^{-3}	9.77×10^{-4}
qpG51	121.6	96.42	527.55	1825	14	800	7.56×10^{-3}	4.80×10^{-4}	9.83×10^{-4}
thetaG11	2.32	8.53	142.53	400	9	1380	1.43×10^{-3}	1.11×10^{-3}	8.31×10^{-5}
thetaG51	71.21	50.08	967.43	1250	11	3240	1.38×10^{-1}	4.03×10^{-4}	9.94×10^{-4}
rs1184	224.86	** * ^m	** * ^m	200	***	***	5.65×10^{-4}	***	***
rs1555	66.6	** * [†]	** * ^m	175	***	***	5.32×10^{-4}	***	***
rs1907	104.61	** * [†]	** * ^m	200	***	***	2.66×10^{-4}	***	***
rs200	12.47	752.27	** * [†]	125	11	***	1.87×10^{-4}	6.11×10^{-4}	***
rs228	12.86	395.24	982.5	125	11	1620	2.15×10^{-4}	6.34×10^{-4}	8.27×10^{-4}
rs35	54.88	919.19	** * [†]	150	12	***	2.48×10^{-4}	3.26×10^{-4}	***
rs365	62.65	** * [†]	** * [†]	175	***	***	3.08×10^{-4}	***	***
rs828	10.84	825.03	** * [†]	125	11	***	1.98×10^{-4}	8.48×10^{-4}	***

¹ with chordal decomposition and clique merging strategy CG2; ² $\max\{\epsilon_1, \epsilon_2, \epsilon_3\}$; [†] time limit reached;
^m out of memory error;

Table 5: Benchmark results for nearest correlation matrix problems.

n	Solve time (s)			Iterations			Max error ²		
	COSMO	MOSEK	SCS	COSMO	MOSEK	SCS	COSMO	MOSEK	SCS
50	0.5	1.89	0.07	25	4	20	2.05×10^{-5}	1.35×10^{-3}	6.18×10^{-7}
100	0.45	35.68	0.18	25	4	20	2.02×10^{-5}	6.26×10^{-3}	4.24×10^{-6}
150	0.39	244.35	0.46	25	4	20	5.15×10^{-5}	8.61×10^{-3}	9.00×10^{-6}
200	0.94	1032.25	0.74	25	4	20	7.59×10^{-5}	3.64×10^{-3}	8.41×10^{-5}
400	1.14	*** [†]	3.07	25	***	20	2.62×10^{-4}	***	8.52×10^{-5}
600	3.05	*** [†]	7.38	25	***	20	1.53×10^{-4}	***	1.01×10^{-4}
800	5.08	*** [†]	13.85	25	***	20	4.03×10^{-4}	***	1.07×10^{-4}
1000	8.43	*** [†]	21.94	25	***	20	8.11×10^{-4}	***	1.40×10^{-4}
1200	12.1	*** [†]	34.58	25	***	20	1.02×10^{-3}	***	1.73×10^{-4}
1400	17.19	*** [†]	49.23	25	***	20	1.02×10^{-3}	***	1.93×10^{-4}
1600	22.69	*** [†]	61.07	25	***	20	8.00×10^{-4}	***	2.21×10^{-4}
1800	29.41	*** [†]	74.0	25	***	20	5.14×10^{-4}	***	2.43×10^{-4}
2000	37.74	*** [†]	101.18	25	***	20	3.31×10^{-4}	***	2.57×10^{-4}

² $\max\{\epsilon_1, \epsilon_2, \epsilon_3\}$; [†] time limit reached

Table 6: Benchmark results for block arrow sparse SDPs with varying number of blocks N_b and block size d .

d	Solve time (s)				Iterations				Max error ²			
	COSMO	COSMO ^{cd}	MOSEK	SCS	COSMO	COSMO ^{cd}	MOSEK	SCS	COSMO	COSMO ^{cd}	MOSEK	SCS
10	12.71	1.22	16.5	56.99	125	175	9	1340	1.50×10^{-4}	5.60×10^{-4}	1.16×10^{-3}	9.01×10^{-4}
12	23.95	2.3	28.72	68.72	125	225	10	1120	2.29×10^{-4}	7.52×10^{-4}	3.65×10^{-5}	5.38×10^{-4}
14	27.4	2.39	41.66	147.72	150	175	10	1780	7.92×10^{-5}	8.60×10^{-4}	6.84×10^{-4}	5.46×10^{-4}
16	36.4	3.6	58.04	254.93	150	275	10	2360	4.76×10^{-5}	5.34×10^{-4}	2.64×10^{-4}	6.91×10^{-4}
18	42.96	4.42	85.81	472.77	150	275	11	3440	2.66×10^{-4}	5.77×10^{-4}	2.55×10^{-4}	3.25×10^{-4}
20	41.13	5.08	112.56	251.39	125	275	11	1460	2.61×10^{-4}	5.35×10^{-4}	6.33×10^{-5}	7.26×10^{-4}
22	50.7	11.47	142.14	520.81	125	700	11	2460	2.87×10^{-4}	5.85×10^{-4}	3.31×10^{-4}	4.86×10^{-4}
24	125.12	10.52	178.75	445.37	275	500	11	1780	7.46×10^{-5}	7.23×10^{-4}	3.57×10^{-4}	5.10×10^{-4}
26	88.74	6.84	220.26	623.46	150	200	11	2060	8.17×10^{-5}	3.27×10^{-4}	2.89×10^{-6}	1.39×10^{-4}
28	98.83	7.47	263.52	1626.82	150	200	11	4660	3.73×10^{-5}	8.93×10^{-4}	2.62×10^{-5}	4.59×10^{-4}
N_b	COSMO	COSMO ^{cd}	MOSEK	SCS	COSMO	COSMO ^{cd}	MOSEK	SCS	COSMO	COSMO ^{cd}	MOSEK	SCS
50	17.31	3.73	28.69	115.36	150	300	10	2540	1.33×10^{-4}	6.28×10^{-4}	2.21×10^{-4}	9.12×10^{-4}
60	21.66	6.4	46.38	217.75	150	475	11	3380	1.42×10^{-4}	8.74×10^{-4}	7.27×10^{-5}	8.81×10^{-4}
70	34.51	9.89	64.8	177.24	175	700	11	2060	4.12×10^{-5}	6.14×10^{-4}	1.72×10^{-5}	8.99×10^{-4}
80	37.22	5.78	85.29	175.38	175	275	11	1540	5.15×10^{-5}	7.13×10^{-4}	2.08×10^{-4}	4.57×10^{-4}
90	63.32	12.85	113.24	234.56	225	550	11	1580	4.80×10^{-5}	1.12×10^{-3}	4.79×10^{-5}	6.40×10^{-4}
100	67.3	25.16	140.81	328.2	200	1100	11	1800	6.38×10^{-5}	9.54×10^{-4}	3.28×10^{-5}	8.59×10^{-4}
110	117.7	39.86	172.99	761.22	275	1650	11	3140	3.78×10^{-5}	6.80×10^{-4}	1.35×10^{-4}	3.53×10^{-4}
120	81.31	29.06	209.96	1191.64	150	1050	11	4620	3.59×10^{-4}	1.07×10^{-3}	3.66×10^{-4}	2.71×10^{-4}
130	115.21	26.61	269.06	1094.53	175	925	12	3580	8.48×10^{-5}	1.31×10^{-3}	8.59×10^{-5}	9.67×10^{-4}
140	114.95	26.87	290.23	** * [†]	150	800	11	***	1.20×10^{-4}	1.92×10^{-3}	4.99×10^{-4}	***

^{cd} with chordal decomposition; ² $\max\{\epsilon_1, \epsilon_2, \epsilon_3\}$; [†] time limit reached

B Appendix

B.1 Projection onto \mathcal{C}_Σ

The projection of a symmetric matrix $S \in \mathbb{S}^n$ onto the set of matrices where the sum of rows and columns each equal to one can be written as the following optimisation problem:

$$\begin{aligned} & \text{minimize} && \frac{1}{2} \|s_p - s\|_F^2 \\ & \text{subject to} && As_p = \mathbf{1}_{2n-1} \end{aligned} \quad (60)$$

where $s = \text{vec}(S)$ is the vectorized matrix, s_p is the projected vector and A is given by:

$$A = [A_r \quad A_c]^\top$$

where A_r is used to constrain the rows of S and A_c is used to constrain the columns of S :

$$A_r = \mathbf{1}_n^\top \otimes I_n \quad A_c = [I_{n-1} \otimes \mathbf{1}_n^\top \quad \mathbf{0}_{n-1 \times n}].$$

Notice that A_c is a $(n-1) \times n$ matrix because the redundant constraint on the last column was removed. By writing down the KKT optimality conditions for (60) we obtain the following equations:

$$As_p = \mathbf{1}_{2n-1}, \quad (61)$$

$$s_p - s + A^\top \eta = 0, \quad (62)$$

with dual variable η . Eliminating s_p and solving for η yields

$$\eta = (AA^\top)^{-1}(As - \mathbf{1}_{2n-1}). \quad (63)$$

The projected vector s_p can be recovered from (62):

$$s_p = s - A^\top \eta. \quad (64)$$

It turns out that the inverse of AA^\top in (63) can be efficiently computed without a factorisation. To see this, form AA^\top and write (63) as:

$$\begin{bmatrix} nI_n & \mathbf{1}_n \mathbf{1}_{n-1}^\top \\ \mathbf{1}_{n-1} \mathbf{1}_n^\top & nI_{n-1} \end{bmatrix} \begin{bmatrix} \eta_1 \\ \eta_2 \end{bmatrix} = \begin{bmatrix} r_1 \\ r_2 \end{bmatrix} \text{ with } \begin{bmatrix} r_1 \\ r_2 \end{bmatrix} = As - \mathbf{1}_{2n-1}, \quad (65)$$

where η and the right-hand side were partitioned in such a way that $\eta_1, r_1 \in \mathbb{R}^n$ and $\eta_2, r_2 \in \mathbb{R}^{n-1}$. Eliminating η_1 from (65), yields:

$$\left(I_{n-1} - \frac{1}{n} \mathbf{1}_{n-1} \mathbf{1}_{n-1}^\top\right) \eta_2 = \frac{1}{n} \left(r_2 - \frac{1}{n} \mathbf{1}_{n-1} \mathbf{1}_n^\top r_1\right) \quad (66)$$

The vector η_2 can be computed by applying the Sherman-Morrison formula to compute the inverse of the matrix on the left:

$$\eta_2 = \frac{1}{n} \left(I_{n-1} + \mathbf{1}_{n-1} \mathbf{1}_{n-1}^\top\right) \left(r_2 - \frac{1}{n} \mathbf{1}_{n-1} \mathbf{1}_n^\top r_1\right). \quad (67)$$

The vector η_1 is then computed by substituting into the upper equation in (65):

$$\eta_1 = \frac{1}{n} \left(r_1 - \mathbf{1}_n \mathbf{1}_{n-1}^\top \eta_2\right). \quad (68)$$

Having computed the elements of the dual variable η , the projected vector s_p is obtained by solving (64).

References

- [ABB⁺99] Edward Anderson, Zhaojun Bai, Christian Bischof, L Susan Blackford, James Demmel, Jack Dongarra, Jeremy Du Croz, Anne Greenbaum, Sven Hammarling, Alan McKenney, et al. *LAPACK Users' guide*. SIAM, 1999.
- [ADV10] Martin S Andersen, Joachim Dahl, and Lieven Vandenbergh. Implementation of nonsymmetric interior-point methods for linear optimization over sparse matrix cones. *Mathematical Programming Computation*, 2(3-4):167–201, 2010.
- [AHMR88] Jim Agler, William Helton, Scott McCullough, and Leiba Rodman. Positive semidefinite matrices with a given sparsity pattern. *Linear Algebra and its Applications*, 107:101–149, 1988.

- [AHO98] Farid Alizadeh, Jean-Pierre A Haeberly, and Michael L Overton. Primal-dual interior-point methods for semidefinite programming: convergence rates, stability and numerical results. *SIAM Journal on Optimization*, 8(3):746–768, 1998.
- [Ali95] Farid Alizadeh. Interior point methods in semidefinite programming with applications to combinatorial optimization. *SIAM Journal on Optimization*, 5(1):13–51, 1995.
- [AV15] M. S. Andersen and L. Vandenberghe. CHOMPACT: A python package for chordal matrix computations, 2015.
- [BBD⁺17] Stephen Boyd, Enzo Busseti, Steve Diamond, Ronald N Kahn, Kwangmoo Koh, Peter Nystrup, Jan Speth, et al. Multi-period trading via convex optimization. *Foundations and Trends® in Optimization*, 3(1):1–76, 2017.
- [BC11] HH Bauschke and PL Combettes. *Convex Analysis and Monotone Operator Theory in Hilbert Spaces*. Springer, 1 edition, 2011.
- [BEGFB94] Stephen Boyd, Laurent El Ghaoui, Eric Feron, and Venkataramanan Balakrishnan. *Linear matrix inequalities in system and control theory*, volume 15. Society for Industrial and Applied Mathematics, 1994.
- [BEKS17] Jeff Bezanson, Alan Edelman, Stefan Karpinski, and Viral B Shah. Julia: A fresh approach to numerical computing. *SIAM Review*, 59(1):65–98, 2017.
- [BGSB17] G. Banjac, P. Goulart, B. Stellato, and S. Boyd. Infeasibility detection in the alternating direction method of multipliers for convex optimization. *Preprint*, 2017.
- [BHH01] Peter Borm, Herbert Hamers, and Ruud Hendrickx. Operations research games: A survey. *Top*, 9(2):139, 2001.
- [BLDR13] Siddharth Barman, Xishuo Liu, Stark C Draper, and Benjamin Recht. Decomposition methods for large scale lp decoding. *IEEE Transactions on Information Theory*, 59(12):7870–7886, 2013.
- [Bor99] B. Borchers. SDPLIB 1.2, a library of semidefinite programming test problems. *Optimization Methods and Software*, 11(1-4):683–690, 1999.
- [BPC⁺11] Stephen Boyd, Neal Parikh, Eric Chu, Borja Peleato, and Jonathan Eckstein. Distributed optimization and statistical learning via the alternating direction method of multipliers. *Foundations and Trends® in Machine Learning*, 3(1):1–122, 2011.
- [CV95] Corinna Cortes and Vladimir Vapnik. Support-vector networks. *Machine Learning*, 20(3):273–297, 1995.
- [D⁺15] Timothy A Davis et al. Suitesparse: A suite of sparse matrix software. *URL <http://faculty.cse.tamu.edu/davis/suitesparse.html>*, 2015.

- [Dan63] GB Dantzig. Linear programming and extensions. *Princeton University Press, Princeton, NT*, 19:63, 1963.
- [DH11] Timothy A Davis and Yifan Hu. The University of Florida sparse matrix collection. *ACM Transactions on Mathematical Software (TOMS)*, 38(1):1–25, 2011.
- [DHL17] Iain Dunning, Joey Huchette, and Miles Lubin. JuMP: A modeling language for mathematical optimization. *SIAM Review*, 59(2):295–320, 2017.
- [EB92] Jonathan Eckstein and Dimitri P Bertsekas. On the Douglas-Rachford splitting method and the proximal point algorithm for maximal monotone operators. *Mathematical Programming*, 55(1):293–318, 1992.
- [Eck89] Jonathan Eckstein. *Splitting methods for monotone operators with applications to parallel optimization*. PhD thesis, Massachusetts Institute of Technology, 1989.
- [Eve63] Hugh Everett. Generalized Lagrange multiplier method for solving problems of optimum allocation of resources. *Operations Research*, 11(3):399–417, 1963.
- [FFN06] K. Fujisawa, M. Fukuda, and K. Nakata. Preprocessing sparse semidefinite programs via matrix completion. *Optimization Methods and Software*, 21(1):17–39, 2006.
- [FKK⁺09] K Fujisawa, S Kim, M Kojima, Y Okamoto, and M Yamashita. User’s manual for SparseCoLO: Conversion methods for sparse conic-form linear optimization problems. *Research Report B-453, Dept. of Math. and Comp. Sci. Japan, Tech. Rep.*, pages 152–8552, 2009.
- [FKMN01] Mitsuhiro Fukuda, Masakazu Kojima, Kazuo Murota, and Kazuhide Nakata. Exploiting sparsity in semidefinite programming via matrix completion I: General framework. *SIAM Journal on Optimization*, 11(3):647–674, 2001.
- [GB14] Pontus Giselsson and Stephen Boyd. Diagonal scaling in Douglas-Rachford splitting and ADMM. In *Decision and Control (CDC), 2014 IEEE 53rd Annual Conference on*, pages 5033–5039. IEEE, 2014.
- [GB15] Pontus Giselsson and Stephen Boyd. Metric selection in fast dual forward-backward splitting. *Automatica*, 62:1–10, 2015.
- [GJSW84] Robert Grone, Charles R Johnson, Eduardo M Sá, and Henry Wolkowicz. Positive definite completions of partial hermitian matrices. *Linear Algebra and its Applications*, 58:109–124, 1984.
- [GM75] Daniel Gabay and Bertrand Mercier. *A dual algorithm for the solution of non linear variational problems via finite element approximation*. Institut de recherche d’informatique et d’automatique, 1975.
- [Gre97] Anne Greenbaum. *Iterative methods for solving linear systems*, volume 17. Society for Industrial and Applied Mathematics, 1997.

- [Hes69] Magnus R Hestenes. Multiplier and gradient methods. *Journal of Optimization Theory and Applications*, 4(5):303–320, 1969.
- [Hig02] Nicholas J Higham. Computing the nearest correlation matrix—a problem from finance. *IMA Journal of Numerical Analysis*, 22(3):329–343, 2002.
- [HRVW96] Christoph Helmberg, Franz Rendl, Robert J Vanderbei, and Henryfa Wolkowicz. An interior-point method for semidefinite programming. *SIAM Journal on Optimization*, 6(2):342–361, 1996.
- [HS12] Michel Habib and Juraj Stacho. Reduced clique graphs of chordal graphs. *European Journal of Combinatorics*, 33(5):712–735, 2012.
- [JPA00] D Johnson, G Pataki, and F Alizadeh. Seventh dimacs implementation challenge: Semidefinite and related problems, 2000. dimacs.rutgers.edu/Challenges/Seventh.
- [KAA⁺15] Alexander Kalinkin, Anton Anders, Roman Anders, et al. Intel® math kernel library PARDISO* for intel® xeon phi tm manycore coprocessor. *Applied Mathematics*, 6(08):1276, 2015.
- [Kar84] Narendra Karmarkar. A new polynomial-time algorithm for linear programming. In *Proceedings of the 16th annual ACM symposium on Theory of Computing*, pages 302–311. ACM, 1984.
- [KKMY11] Sunyoung Kim, Masakazu Kojima, Martin Mevissen, and Makoto Yamashita. Exploiting sparsity in linear and nonlinear matrix inequalities via positive semidefinite matrix completion. *Mathematical programming*, 129(1):33–68, 2011.
- [Kru56] J. B. Kruskal. On the shortest spanning subtree of a graph and the traveling salesman problem. *Proceedings of the American Mathematical society*, 7(1):48–50, 1956.
- [LDGL20] Benoit Legat, Oscar Dowson, Joaquim Dias Garcia, and Miles Lubin. MathOpt-Interface: a data structure for mathematical optimization problems. *arXiv preprint arXiv:2002.03447*, 2020.
- [MCIL71] A Miele, EE Cragg, RR Iyer, and AV Levy. Use of the augmented penalty function in mathematical programming problems, part 1. *Journal of Optimization Theory and Applications*, 8(2):115–130, 1971.
- [MCL71] A Miele, EE Cragg, and AV Levy. Use of the augmented penalty function in mathematical programming problems, part 2. *Journal of Optimization Theory and Applications*, 8(2):131–153, 1971.
- [Meh92] Sanjay Mehrotra. On the implementation of a primal-dual interior point method. *SIAM Journal on Optimization*, 2(4):575–601, 1992.

- [MHL13] Daniel K Molzahn, Jesse T Holzer, Bernard C Lesieutre, and Christopher L DeMarco. Implementation of a large-scale optimal power flow solver based on semidefinite programming. *IEEE Transactions on Power Systems*, 28(4):3987–3998, 2013.
- [Mit] Hans Mittelmann. Benchmarks for optimization software. <http://plato.asu.edu/bench.html>. Accessed: 2020-06-22.
- [MM99] Istvan Maros and Csaba Mészáros. A repository of convex quadratic programming problems. *Optimization Methods and Software*, 11(1-4):671–681, 1999.
- [MMLC72] Angelo Miele, PE Moseley, AV Levy, and GM Coggins. On the method of multipliers for mathematical programming problems. *Journal of Optimization Theory and Applications*, 10(1):1–33, 1972.
- [MOS17] MOSEK, Aps. The MOSEK optimization toolbox for MATLAB manual. Version 8.0 (revision 57), 2017.
- [NFF⁺03] K. Nakata, K. Fujisawa, M. Fukuda, M. Kojima, and K. Murota. Exploiting sparsity in semidefinite programming via matrix completion II: Implementation and numerical results. *Mathematical Programming*, 95(2):303–327, 2003.
- [OCPB16] B. O’Donoghue, E. Chu, N. Parikh, and S. Boyd. Conic optimization via operator splitting and homogeneous self-dual embedding. *Journal of Optimization Theory and Applications*, 169(3):1042–1068, jun 2016. arXiv: [1312.3039](https://arxiv.org/abs/1312.3039) [math.OA].
- [PB⁺14] Neal Parikh, Stephen Boyd, et al. Proximal algorithms. *Foundations and Trends® in Optimization*, 1(3):127–239, 2014.
- [Pow69] Michael JD Powell. A method for nonlinear constraints in minimization problems. *Optimization*, pages 283–298, 1969.
- [PS90] A. Pothén and C. Sun. Compact clique tree data structures in sparse matrix factorizations. *Large-Scale Numerical Optimization*, pages 180–204, 1990.
- [RG19] Nikitas Rontsis and Paul J Goulart. Optimal approximation of doubly stochastic matrices. *arXiv preprint arXiv:1910.05295*, 2019.
- [RGN19] Nikitas Rontsis, Paul J Goulart, and Yuji Nakatsukasa. Efficient semidefinite programming with approximate admm. *arXiv preprint arXiv:1912.02767*, 2019.
- [RHD⁺14] Suhas SP Rao, Miriam H Huntley, Neva C Durand, Elena K Stamenova, Ivan D Bochkov, James T Robinson, Adrian L Sanborn, Ido Machol, Arina D Omer, Eric S Lander, et al. A 3d map of the human genome at kilobase resolution reveals principles of chromatin looping. *Cell*, 159(7):1665–1680, 2014.
- [Roc70] Ralph Tyrrell Rockafellar. *Convex analysis*. Princeton University Press, 1970.
- [Roc76] R Tyrrell Rockafellar. Monotone operators and the proximal point algorithm. *SIAM Journal on Control and Optimization*, 14(5):877–898, 1976.

- [Rui01] Daniel Ruiz. A scaling algorithm to equilibrate both rows and columns norms in matrices. Technical report, 2001.
- [SAV14] Y. Sun, M. S. Andersen, and L. Vandenberghe. Decomposition in conic optimization with partially separable structure. *SIAM Journal on Optimization*, 24(2):873–897, 2014. arXiv: [1306.0057](https://arxiv.org/abs/1306.0057) [math.OC].
- [SBG⁺18] B. Stellato, G. Banjac, P. Goulart, A. Bemporad, and S. Boyd. OSQP: An Operator Splitting Solver for Quadratic Programs. *ArXiv e-prints*, 2018.
- [SGK⁺10] Olaf Schenk, K Gärtner, G Karypis, S Röllin, and M Hagemann. Pardiso solver project. URL: <http://www.pardiso-project.org>, 2010.
- [Stu99] Jos F Sturm. Using SeDuMi 1.02, a MATLAB toolbox for optimization over symmetric cones. *Optimization Methods and Software*, 11(1-4):625–653, 1999.
- [TTT99] Kim-Chuan Toh, Michael J Todd, and Reha H Tütüncü. SDPT3 - A MATLAB software package for semidefinite programming, version 1.3. *Optimization Methods and Software*, 11(1-4):545–581, 1999.
- [UMZ⁺14] Madeleine Udell, Karanveer Mohan, David Zeng, Jenny Hong, Steven Diamond, and Stephen Boyd. Convex optimization in Julia. *SC14 Workshop on High Performance Technical Computing in Dynamic Languages*, 2014.
- [VA⁺15] Lieven Vandenberghe, Martin S Andersen, et al. Chordal graphs and semidefinite optimization. *Foundations and Trends® in Optimization*, 1(4):241–433, 2015.
- [Van95] Robert J. Vanderbei. Symmetric quasidefinite matrices. *SIAM Journal on Optimization*, 5(1):100–113, 1995.
- [WN99] Stephen Wright and Jorge Nocedal. Numerical optimization. *Springer Science*, 35, 1999.
- [Wol59] Philip Wolfe. The simplex method for quadratic programming. *Econometrica: Journal of the Econometric Society*, pages 382–398, 1959.
- [Wri97] Stephen J Wright. *Primal-dual interior-point methods*, volume 54. Society for Industrial and Applied Mathematics, 1997.
- [Yan81] M. Yannakakis. Computing the minimum fill-in is NP-complete. *SIAM Journal on Algebraic Discrete Methods*, 2(1):77–79, 1981.
- [ZFP⁺19] Y. Zheng, G. Fantuzzi, A. Papachristodoulou, P. Goulart, and A. Wynn. Chordal decomposition in operator-splitting methods for sparse semidefinite programs. *Mathematical Programming*, pages 1–44, 2019. arXiv: [1707.05058](https://arxiv.org/abs/1707.05058) [math.OC].
- [ZS07] Ron Zass and Amnon Shashua. Doubly stochastic normalization for spectral clustering. In *Advances in neural information processing systems*, pages 1569–1576, 2007.